Numerically Efficient Parallel Algorithms

Prepared for the

U.S. Department of Energy
Office of Electricity Delivery and Energy Reliability

Under Cooperative Agreement No. DE-FC26-06NT42847
Hawai‘i Distributed Energy Resource Technologies for Energy Security

Subtask 10.3 Deliverable 1
Report on System Simulation using High Performance Computing

Prepared by

New Mexico Tech
New Mexico Institute of Mining and Technology

Submitted to

Hawai‘i Natural Energy Institute
School of Ocean and Earth Science and Technology
University of Hawai‘i

October 2012

Acknowledgement: This material is based upon work supported by the United States Department of Energy under Cooperative Agreement Number DE-FC-06NT42847.

Final Report for Task One

Project:	Application of High Performance Computing to Electric Power System Modeling, Simulation and Analysis
Task One:	Numerically Efficient Parallel Algorithms
Sponsor:	Hawaii Natural Energy Institute, University of Hawaii
Date:	June 8, 2011

Abstract

This report presents an approach based upon probabilistic load flow to study the effect of wind generation and variation in loads on an electric power grid. A probabilistic approach was adopted due to the variation and uncertainty associated with wind generation and power consumption. As the modern power grid advances and evolves to accommodate larger amounts of renewable generation, such as wind farms, statistical analysis becomes an appropriate approach to study such systems. Probabilistic load flow is based upon standard load flow in which complex power balance equations are solved, but instead of one solution a distribution of solutions is found by taking the randomness of wind generation and loads into consideration.

A new method of selecting random variables from historical data is implemented by finding the times of day where power generated or consumed is above or below a given threshold, and correlating the data to incorporate the effects of sites that are geographically close to each other. This is contrast to other methods where data have been separated into monthly, weekday and weekend intervals. By breaking up the loads into these smaller intervals, a narrower (lower variance) distribution is created from which random load and wind speed data are selected, and in turn creates narrower distributions for variable outputs. The IEEE 24-bus test system was utilized to demonstrate the proposed approach and impact of taking multiple intervals when selecting random variable.

Results are presented for a basic load flow implementation from which histograms were computed for voltages, phase angles, line powers and slack bus fluctuations. This method results in one generator picking up the entire power mismatch of the system. To create more realistic scenarios, economic dispatch was implemented to allow the power mismatch between wind generation and consumption to be distributed among multiple generators based on the minimization of the total cost to run all generators. Results of the study are distributions for all quantities (magnitudes and phase angles of voltages, real and reactive power at generators, loads, and line powers) that can be used for finding the likelihood of low-voltage conditions, overloaded lines, etc, which are useful for system planning and studies. These distributions show that by taking specific intervals of wind and load data separated by size, which correlates to specific times of the day, the variance of the solution tends to decrease. This implies more conclusive results. In addition, the variance of the power output of the generators under economic dispatch gives a measure of how widely their power outputs will need to swing and if there are any cases where more generation would need to be installed.

Contents

List of Tables

List of Figures

1 Introduction

Most countries have established renewable energy mandate laws that require a specified percentage of the total energy production to come from renewable sources by certain dates. The increase in power demand, desire to decrease green house gases, and the depletion and continuous price fluctuations in fossil fuels are the main contributing factors for the goal to transition from traditional generation towards renewable energy. Some of the more popular choices in renewable energy are intermittent sources such as wind and solar energy. Wind energy has gained popularity for its relatively high potential output vs. cost ratio.

Intermittent energy sources add more uncertainty to the power grid and thus require statistical/probabilistic approaches for analysis and planning. One such method is probabilistic load flow which originated in the 1970's by assuming the statistical nature of load buses as independent random variables [1, 2]. Numerous methods and advancements have been applied to probabilistic load flow including the brute force Monte Carlo simulation [3], the simplified point estimation and Fast Fourier Transform (FFT) techniques [4, 5], as well as self learning algorithms such as fuzzy logic [6]. Techniques such as point estimation and FFT are computationally inexpensive but are less accurate than using a large number of Monte Carlo simulations [3].

With the increase in wind farm penetration on the grid, newer Monte Carlo simulations are used to develop correlated loads and wind farms using the multivariate distribution to select random variables intelligently [7]. In a small area it is likely that if wind is blowing at one site, then a second nearby site has a similar wind speed magnitude and thus a dependency exists between the random variables. It is also understood that load buses within a close proximity and time zone will have a similar behavior [8]. There are many contributing factors that influence load buses. In reference [8], Allan and DeSilva explain that social and environmental factors are the primary contributors to these phenomena. For example, high temperatures show an increase in reactive power caused from the motors in air conditioners while low temperatures show an increase in active power caused from the resistance in electric heating.

Probabilistic load flow computes multiple deterministic, steady state solutions assuming perfect generator governor, frequency, and power control. In terms of wind turbines, the controllers include instantaneous optimal pitch, yaw, and power factor or voltage control. The dynamics of all generator turbines, and load buses are ignored or assumed perfect instantaneous transitions between steady state equilibrium. In other words, steady state analysis displays a snapshot of the grid's equilibrium state for every bus on the transmission level of the system. Power companies care about steady state solutions as basic understanding of the behavior of the system and as a planning tool. Steady state analysis determines if the equilibrium states are within allowed criteria, where as dynamical analysis is a tool used to check for stability.

Isolated systems have been studied over the last 20 years [9], with results showing unique problems that larger interconnected grids don't notice. These include frequency response and transient stability issues, resulting from lack of inertia on the power grid [10]. The most popular wind turbine models purchased in today's market are the Doubly Fed Induction Generator (DFIG) and Full Converter [11]. Both models disconnect their inertia from the grid and pose major problems due to its partial electrical interconnection for isolated systems when displacing traditional generation. Typically wind farms are placed in windy areas far from load buses, where the long distance power transfer through congested transmission lines can become a problem. Therefore, there are limitations to the maximum amount of wind energy that can be integrated into an isolated system [9].

Transmission line power calculations are an essential piece of information that helps determine the integrity of the overall system performance. The line power values are compared against the line load-ability and thermal line limits to determine the remaining capacity/congestion. Probabilistic load flow can be used to compare the values of multiple simulations and determine what percentage of the solutions have line powers near or above these limits. If the line powers are at one of the limits a relatively high percentage of the time, it can be assumed that the line will get disconnected to prevent damage to connected equipment and the line itself. During this process all power on the disconnected line transfers over to neighboring transmission lines [12].

Cascading line failure analysis can be performed by removing the faulted line and performing probabilistic load flow simulations for the new system. This process is repeated by removing new transmission lines that have reached their maximum line power stability limit or thermal values. Probabilistic load flow simulations are then performed to determine if the remaining transmission lines are within their respected limits. If this is not possible, power companies can look at these results and determine the best location to perform a load shed or redispatch generation. In the United States, transmission lines are owned by private investors, according to the Federal Energy Regulatory Commission (FERC) orders 888 and 889 [13], where investors monitor their transmission lines and utilize these results to make decisions if and where new transmission lines need to be added.

Others who have studied probabilistic load flow with large amounts of wind energy have emphasized the use of the multivariate distribution as the basis of selecting random variables. One author explains how the Cornish-Fisher expansion is used to create a distribution when encountering non-Gaussian correlated dependent random variables for forecasting stochastic power in power systems [7]. By defining cumulants and moments through the Corner-Fisher expansion the author explains that the random variable selection for predicting wind farm power output is more accurate than older methods. Another source uses data correlation to differentiate comonotonicity/dependent variables and countermonotonicity/independent variables, and finding zones where each method is beneficial [14]. For smaller systems the input variables have a strong dependence and thus the dependent random variable selection is more accurate. For larger systems the random variable selection falls somewhere in between dependent and independent random variable depending on geographical locations. A newer random variable selection technique is thus developed to select wind farm power output based on the clusters of high correlated and less correlated regions.

The work in this report entails the idea of partitioning load bus data based on time intervals containing upper and lower threshold values of the load demand. This will be further partitioned by weekdays/weekends and season to account for the different temperatures and electrical devices in use. Wind data will be chosen within the same time intervals to show the impact of wind farms when load buses are approaching these upper and lower threshold values. This will provide a narrower variance between load buses and wind farms and thus a more accurate random variable selection. New Mexico Tech's super computer, Exemplar, will run multiple task parallel Monte Carlo deterministic load flow simulations with the new method of selecting random variables. Lastly economic dispatch is implemented in order to simulate a more realistic system where the generators respond according to the price of each generator's fuel. The results will be in the form of histograms containing data for every run.

The report is arranged as follows. Section two will give a background discussion on deterministic and probabilistic load flow, the methods used for solving the power flow equations, and the process of selecting and using the statistical data. Section three will explain the process of this work and the various tests performed in more detail. The tests include the comparison of using time intervals vs daily and non load threshold interval data, and load flow vs economic dispatch solutions. Section four will discuss the statistical results of bus voltages, line powers, phase angle differences, and generator fluctuations. Lastly chapter five will wrap things up with a conclusion.

2 Background

2.1 Electric Power System

Electric power systems are the largest interconnected critical infrastructures in the world. For A.C. electricity, electric power is produced at generators where it is transferred by cable to a switchyard containing transformers and circuit breakers. Voltage is the force that moves electricity, and these transformers increase the voltage to values sometimes as high as $765kV$. Voltage is increased to allow the electricity to travel long distances and reduce line losses. The circuit breakers are used to connect to other transmission equipment and to more switchyards. The connection between multiple switchyards is considered a power system. If one generator was to go down, the connection between the switchyards would allow power to travel to the locations the off-line generator was supporting. Circuit breakers are also used as protective devices by disconnecting transmission lines in the presence of currents above or below the connecting equipments rating. Before the electricity reaches the load areas, it passes through a substation which contains more transformers that are used to lower the voltage, typically between 2kV and 33kV. The power on the lines coming from the substation is routed to the load areas in need of power, and lowered once more to 120V with one final transformer typically located on a power pole.

Generators, loads, transmission lines, switchyards, substations, transformers, system protection and control devices all make up the electric power grid, and work in synchronization to produce power, oscillating at 60Hz, with a 120V output nationwide in the United States. A.C. electricity is used for its economical and ease of transforming voltages. A bus is typically referred to as a substation or more generally a point between interconnected equipment. If the system frequencies, voltages, line powers, etc. deviate from their nominal values for a short period of time, damage can occur to the connected devices as the equipment is designed to operate near these rated values.

2.2 Deterministic Load Flow

An initial approximation of how an electric power system behaves is achieved through calculating the power balance equations at every bus, also known as deterministic load flow. The power balance equations model the transmission level of the power grid in sinusoidal steady state, ignoring the transient characteristics of the transmission lines, loads, and generators. This study will also assume that the three phases of the transmission level are balanced and thus a one line diagram can be used to represent the power grid. Deterministic load flow assumes constant generated power, absorbed load, line powers, bus voltages and angles, and equations have the following algebraic form at bus k [15]

$$
\begin{aligned}
S_k &= P_k + jQ_k && (1)\\
&= V_k I_k^* = V_k e^{j\alpha_k} I_k e^{j\beta_k} = V_k^{\angle \alpha_k} I_k^{*\angle \beta_k} = V_k I_k^{\angle(\alpha_k - \beta_k)} && (2)\\
&= |V_k||I_k| cos(\alpha_k - \beta_k) + j|V_k||I_k| sin(\alpha_k - \beta_k) && (3)
\end{aligned}
$$

where S is the complex power consisting of real (P) and reactive (Q) power, k is the bus number, V_k is the bus voltage, I_k denotes the current injected into bus k, $()^*$ denotes the complex conjugate of the argument, $\angle$ represents the phase of the voltage or current, α and β are the voltage and current angles respectively. Equation 2.2 displays the exponential and phaser forms of the complex power, and equation 2.3 is the rectangular representation of the complex power derived from Euler's formula $e^{jx} = cos(x) + jsin(x)$. To maintain power balance at any bus k the complex power has the form

$$
\begin{aligned}
S_k = V_k \sum_{m=1}^{n} |Y_{bus,km}| V_m \cos(\delta_k - \theta_{km} - \delta_m) \\
+ jV_k \sum_{m=1}^{n} |Y_{bus,km}| V_m \sin(\delta_k - \theta_{km} - \delta_m)
\end{aligned} \tag{4}
$$

where n is the total number of buses, δ is the voltage angle, Y_{bus} is the admittance, and $Y_{bus,km}$ is an element of of Y_{bus} at row k, and column m. θ_{km} is the admittance (Y_{bus}) angle of element $Y_{bus,km}$, voltages V_k and V_m are the magnitudes of the bus voltages. The sign of the bus power in equation 2.4 depends on whether the power is injected or received at the bus. The line admittance Y is defined to be the inverse of the line impedances Z,

$$
\begin{aligned}
Z &= R + jX && (5)\\
Y &= \frac{1}{R + jX} = G + jB && (6)
\end{aligned}
$$

where R is the resistance, X is the reactance, G is the conductance and B is the susceptance. For a grid system the admittances are placed in matrix form to relate all complex voltages to currents injected at all buses, and is typically sparse. The admittance matrix describes current-balance at each bus:

$$
\begin{bmatrix}
Y_{bus,11} & Y_{bus,12} & Y_{bus,13} & \cdots & Y_{bus,1n} \\
Y_{bus,21} & Y_{bus,22} & Y_{bus,23} & \cdots & Y_{bus,2n} \\
Y_{bus,31} & Y_{bus,32} & Y_{bus,33} & \cdots & Y_{bus,3n} \\
\vdots & \vdots & \vdots & \ddots & \vdots \\
Y_{bus,n1} & Y_{bus,n2} & Y_{bus,n3} & \cdots & Y_{bus,nn}
\end{bmatrix}
\begin{bmatrix} V_1 \\ V_2 \\ V_3 \\ \vdots \\ V_n \end{bmatrix}
=
\begin{bmatrix} I_1 \\ I_2 \\ I_3 \\ \vdots \\ I_n \end{bmatrix} \tag{7}
$$

and is formulated with the diagonal elements $Y_{bus,kk}$, being the sum of the admittances connected to bus k, the off-diagonal elements $Y_{bus,km}$, are the negative sum of the admittances connected between buses k and m, and n is the total number of buses. The admittance matrix for the 24-bus test system in this study can be found in Appendix 2. The admittances are computed assuming the pi equivalent model of a transmission line shown in Figure 2.1 and equations 2.8 through 2.11. the current and power equations of the pi-equivalent model. The pi-equivalent model is used for its ability to account for the capacitance between the transmission lines and the ground for different line lengths.

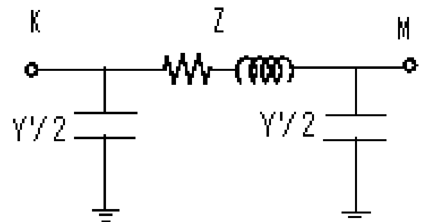

Figure 2.1: PI-Equivalent model.

$$I1_{km} = \frac{V_k - V_m}{Z} + V_k \frac{Y'}{2} \tag{8}$$
$$I2_{mk} = \frac{V_m - V_k}{Z} + V_m \frac{Y'}{2} \tag{9}$$
$$S1_{km} = V_k I_{km}^* \tag{10}$$
$$S2_{mk} = V_m I_{mk}^* \tag{11}$$

where k is the transmitting bus side and m is receiving bus side, Z is the line impedance, $Y'/2$ is the shunt admittance, $S1_{km}$ and $I1_{km}$ are the injected side line power and current and $S2_{mk}$ and $I2_{mk}$ are the received side line power and current. Subscripts km and mk represent the direction of the power and current. Transmission lines have a maximum power (load-ability) and thermal limit allowed in order to maintain a stable system. The max power occurs at a phase angle $(\delta) = 90^o$. For thermal limits the amount of power allowed varies with each system according to the characteristics and parameters of the steel and aluminum cables that make up the transmission level of the grid. The line power and thermal limits are computed and compared with the line tolerances, the equations are:

$$P_{max} = V_k \sum_{m=1}^{n} Y_{bus,km} V_m \cos(\delta_k - \theta_{km} - \delta_m) \tag{12}$$
$$S_{thermal} = V_k I_{km} \tag{13}$$

All grid powers, voltages, currents, and admittances are per unitized to have a common basis:

$$p.u. = \frac{actual\ value}{base\ value} \tag{14}$$

in order to remove the voltage difference on both sides of the transformers and to create values that are easier to compare and plot. The base value for the complex power is chosen by the user and then divides into each of the remaining generator powers to ease the burden of computations with large numbers. The base value for the voltage is also selected by the user. The value is typically selected by calculating the ratio of the voltages on both sides of a transformer and setting that equal to the ratio of the transformer's voltage ratings. By following the above two criteria, the impedances on either side of the transformer remains the same and completely removes the transformer from the system. The currents, impedances, and admittances can be per-unitized as a consequence of selecting the complex power and voltage base.

The complex power equations at each bus can be broken up into real and imaginary parts:

$$P_k = V_k \sum_{m=1}^{n} Y_{bus,km} V_m \cos(\delta_k - \delta_m - \theta_{km}) \tag{15}$$

$$Q_k = V_k \sum_{m=1}^{n} Y_{bus,km} V_m \sin(\delta_k - \delta_m - \theta_{km}) \tag{16}$$

At bus k, P_k and Q_k are the two governing algebraic equations and contain four unknown variables: P_k, Q_k, V_k, and, δ_k. Since there are two equations and four unknown quantities, choices need to be made as to known and unknown quantities such that the equations can be solved. These choices are based on what is connected at each bus. If a generator is connected to the bus, the bus is considered either a slack or PV bus. The slack bus is responsible for providing the remaining real and reactive generation needed to solve the power balance equations. There is typically only one slack bus per system and is usually connected to the largest generator. Since this is the case, and the voltages are in per unit values, the voltage can be assumed 1 p.u. Usually this value is slightly above 1 p.u. to account for decreasing voltage levels away from the generator. The angle at the slack bus is an unknown quantity; however power engineers are only concerned with the angle difference between buses. Therefore the slack bus angle must be set to a constant value (zero) and the angle differences are found at the other buses with respect to the slack bus. A PV bus assumes that the connected generator has perfect real power and voltage control through means such as governor and automatic voltage regulator control. The δ's and Q's remain to be solved. Lastly the PQ buses assume known values for the loads. These values can be determined through data based on hourly, daily, monthly, and annually gathered statistics. There are now two equations and two unknown quantities for every bus which can now be solved with an iterative process such as the Newton-Raphson method since they are nonlinear.

2.2.1 The Newton-Raphson Method

The Newton-Raphson method is an iterative process that quickly converges to a solution. Mathematically Newton-Raphson has the form:

$$p_n = p_{n-1} - \frac{f\left(p_{n-1}\right)}{f'\left(p_{n-1}\right)} \quad for \;\; n \geq 1 \tag{17}$$

where p_0 is the initial guess, and value that the function and its derivative is evaluated at for the first iteration. The answer from that iteration is the evaluation point for the next iteration. The process is repeated until p_n is within a specified tolerance. Equation 2.17 is derived from the Taylor series expansion, i.e.

$$0 = f\left(\overline{x}\right) + \left(p - \overline{x}\right) f'\left(\overline{x}\right) + \frac{\left(p - \overline{x}\right)^2}{2} f''\left(\xi\left(p\right)\right) \tag{18}$$

where p is the desired root of the equation, $\overline{x}$ is the approximation of the root, and ξ is the error term. Being that the error term is the second degree position of the Taylor series expansion polynomial guarantee a close to quadratic rate of convergence. For the power system the process is performed as follows: create a vector of known quantities $\overline{y}$, taken from $\overline{P}$ and $\overline{Q}$, a vector of unknown quantities $\overline{x}$ containing the δ's and V's, and a vector function $\overline{f}(x)$ representing the power balance equations, containing the known $P's$ and $Q's$ with the unknown $V's$ and δ's, i.e.

$$\overline{y} = \begin{bmatrix} \overline{P} \\ \overline{Q} \end{bmatrix} \quad \overline{x} = \begin{bmatrix} \overline{\delta} \\ \overline{V} \end{bmatrix} \quad \overline{f}(\overline{x}) = \begin{bmatrix} \overline{P}(\overline{x}) \\ \overline{Q}(\overline{x}) \end{bmatrix} \tag{19}$$

The next step is to form the Jacobian matrix. The Jacobian is found in the second term of the Taylor series expansion, where the Jacobian $J = f'$, and consists of partial derivatives of the real and reactive powers with respect to bus voltage's and δ's:

$$J = \begin{bmatrix} \frac{\partial \overline{P}}{\partial \overline{\overline{\delta}}} & \frac{\partial \overline{P}}{\partial \overline{\overline{V}}} \\ \frac{\partial \overline{Q}}{\partial \overline{\overline{\delta}}} & \frac{\partial \overline{Q}}{\partial \overline{\overline{V}}} \end{bmatrix} = \begin{bmatrix} J1 & J2 \\ J3 & J4 \end{bmatrix} \tag{20}$$

This can be broken into on and off diagonal elements by taking appropriate derivatives of the power balance equations.

The on-diagonal elements are:

$$J1 = \frac{\partial P_k}{\partial \delta_m} = -V_k \sum_{m \neq k}^{n} V_m Y_{bus,km} sin(\delta_k - \delta_m - \theta_{km}) \tag{21}$$

$$J2 = \frac{\partial P_k}{\partial V_n} = 2V_k Y_{bus,kk} cos(\theta_{kk}) + \sum_{m \neq k}^{n} V_m Y_{bus,km} cos(\delta_k - \delta_m - \theta_{km}) \tag{22}$$

$$J3 = \frac{\partial Q_k}{\partial \delta_m} = V_k \sum_{m \neq k}^{n} V_m Y_{bus,km} cos(\delta_k - \delta_m - \theta_{km}) \tag{23}$$

$$J4 = \frac{\partial Q_k}{\partial V_m} = -2V_k Y_{bus,kk} sin(\theta_{kk}) + \sum_{m \neq k}^{n} V_n Y_{bus,km} cos(\delta_k - \delta_m - \theta_{km}) \tag{24}$$

and the off-diagonal elements are:

$$J1 = \frac{\partial P_k}{\partial \delta_m} = V_k V_m Y_{bus,km} sin(\delta_k - \delta_m - \theta_{km}) \tag{25}$$

$$J2 = \frac{\partial P_k}{\partial V_m} = V_k Y_{bus,km} cos(\delta_k - \delta_m - \theta_{km}) \tag{26}$$

$$J3 = \frac{\partial Q_k}{\partial \delta_m} = -V_k V_m Y_{bus,km} cos(\delta_k - \delta_m - \theta_{km}) \tag{27}$$

$$J4 = \frac{\partial Q_k}{\partial V_m} = V_k Y_{bus,km} sin(\delta_k - \delta_m - \theta_{km}) \tag{28}$$

The Jacobian matrix can be reduced to make it computationally efficient based on the number of each type of bus. Since there is only one slack bus at which the voltage and angle are known, the first row and column of the Jacobian matrix can be eliminated. At every PV bus, the voltages are known and thus M more rows and columns can be removed, where M is the number of PV buses. Newton-Raphson method uses the following equation to solve for the unknown quantities:

$$\begin{bmatrix} \Delta P \\ \Delta Q \end{bmatrix} = \begin{bmatrix} J1 & J2 \\ J3 & J4 \end{bmatrix} \begin{bmatrix} \Delta \delta \\ \Delta V \end{bmatrix} \tag{29}$$

The last step of the process uses the following equations to update $\overline{x}$ until the magnitude of $\Delta\overline{x}$ is within a specified tolerance, for this study the tolerance is set at 10^{-6}.

$$\Delta\overline{y} = \overline{y} - \overline{f}(\overline{x}) \tag{30}$$

$$\Delta\overline{x} = J^{-1}\Delta\overline{y} \tag{31}$$

$$\overline{x}_{i+1} = \overline{x}_i + \Delta\overline{x} \tag{32}$$

After the V's and δ's are solved, the P's and Q's can be solved for the slack bus, and the Q's can be solved for the PV buses. The Newton-Raphson method is best understood with Figure 2.2.

An initial guess is made on $f(\overline{x})$. A tangent line is constructed from that point. The point the tangent line crosses the x-axis is used for the second iteration and evaluated on $f(\overline{x})$. Another tangent line is constructed and the process repeats until the magnitude of Δx is within the users desired tolerance.

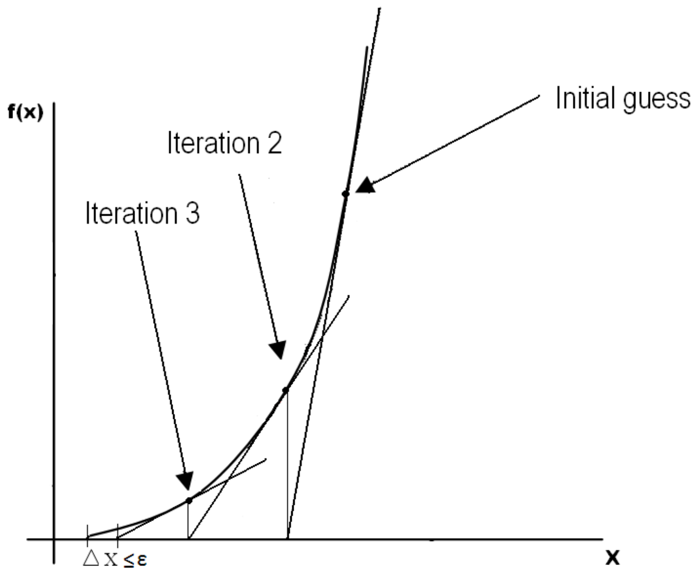

Figure 2.2: Newton-Raphson method of convergence.

2.3 IEEE Test System

The IEEE 24-bus test system shown in Figure 2.3, was chosen to help demonstrate the effects of adding a considerable amount of intermittent source penetration to a smaller islanded power grid. The IEEE 24-bus test system has 10 generators, 1 condenser, 17 loads, and 38 transmission lines. A condenser is a generator that only generates reactive power. IEEE 24-bus test system data comes in IEEE common format which contains transmission line connection information, line parameters, generator and load active and reactive power values, and voltage magnitudes and phase angles. For this project randomly selected, scaled up load data from two small New Mexico towns is placed inside the 17 load positions, two generators are replaced with randomly selected wind turbine power data, the condenser is assumed a negative load, and line parameters for wind turbine buses are changed to the typical GE wind farm connection impedance, $R = 0.0375\ \Omega$ and $X = 0.3750\ \Omega$. Parameters for the system can be found in [16]

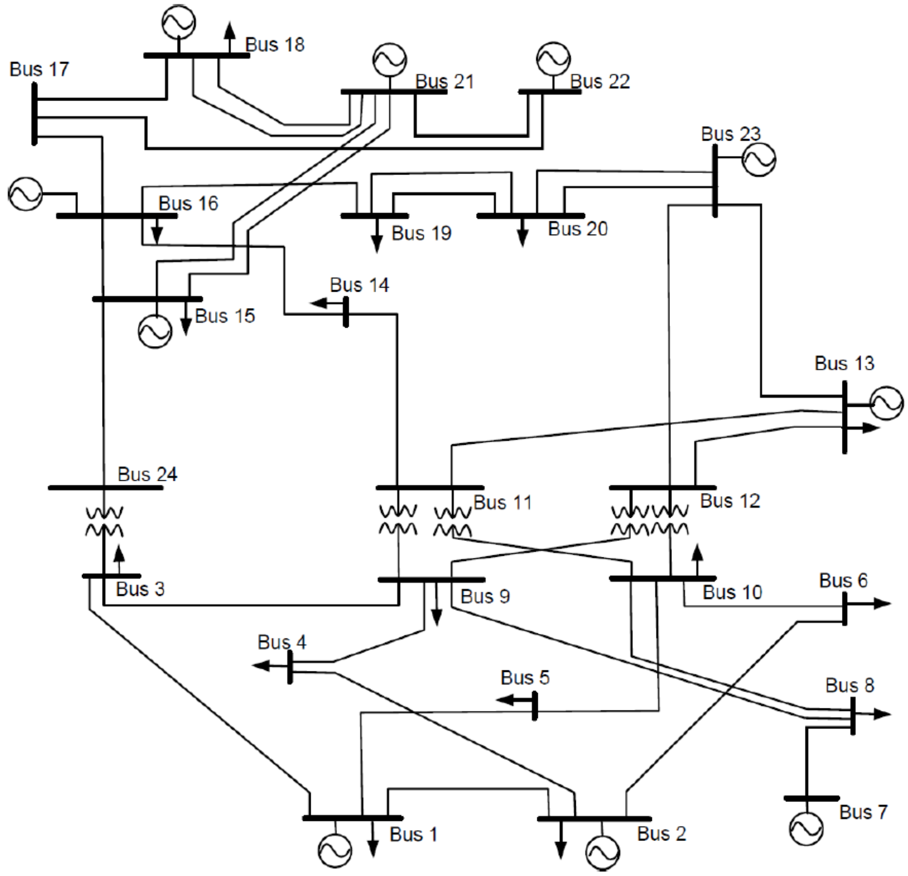

Figure 2.3: IEEE 24-bus test system

2.3.1 Economic Dispatch

Economic dispatch is a more realistic method of studying load flow, by allowing more than one generator to react to grid fluctuations. Cost functions are assigned to each generator with coefficient size proportional to the price of fuel of each generator per hour. The cost functions have the form:

$$
\begin{aligned}
C_T &= \sum_{i=1}^{N} C_i && (33)\\
&= C_1(P_1) + C_2(P_2) + ... + C_N(P_N) && (34)\\
&= (A_1P_1 + B_1P_1^2) + (A_2P_2 + B_2P_2^2) + ... + (A_NP_N + B_NP_N^2) && (35)
\end{aligned}
$$

where A and B are cost function coefficients and $P_1...P_N$ are the generator powers. In 2008 the United States average price of each type of fuel in dollars per million BTU is found on the EIA website, http://www.eia.gov. The ratio between each price determined the coefficients of the cost function. The prices are:

Fuel	Coal	Petroleum	Nuclear	Hydro
$\frac{\$}{MBTU}$	2.09	13.48	0.47	1.88

Table 2.1: Price of fuel per million BTU

The generators of the IEEE 24-bus test system use the following fuel and cost function coefficients:

Generator No	Bus No	Fuel Type	A	B
1	13	Oil	16	28e-3
2	2	Oil	14	25e-3
3	7	89%Coal/11%Oil	8	17e-3
4	23	Coal	6	9e-3
5	15	89%Coal/11%Oil	7	14e-3
6	18	Nuclear	3	10e-3
7	21	Nuclear	3	10e-3
8	22	Hydro	5	12e-3

Table 2.2: Generator fuel type and cost function coefficients

The generators are then subjected to a maximum and minimum power output. The maximum power is assumed 10% higher than the original load flow values, and the minimum is assumed 50% below the original values so as to not allow the generators to perform a cold start. However the three most expensive generators can shut down completely in this study. Plotting the cost functions, shown in Figure 2.4, reveals the order to run each generator at the lowest price as power increases. Taking the derivative of the cost function with respect to power yields price of each generator per megawatt hour. To minimize the price of the total generation, take the Laplacian of dC/dP, set the derivatives equal to each other and solve for λ, i.e.:

$$\frac{dC_1}{dP_1} = \frac{dC_2}{dP_2} = ... = \frac{dC_N}{dP_N} = \lambda \tag{36}$$

λ can be solved by breaking up the cost function coefficients into β and γ components, where

$$\beta = [A_1, A_2, ..., A_N] \tag{37}$$

$$\gamma = [B_1, B_2, ..., B_N] \tag{38}$$

and plugging into

$$\lambda = \frac{P_T + \sum \frac{\beta_i}{2\gamma_i}}{\sum \frac{1}{2\gamma_i}} \tag{39}$$

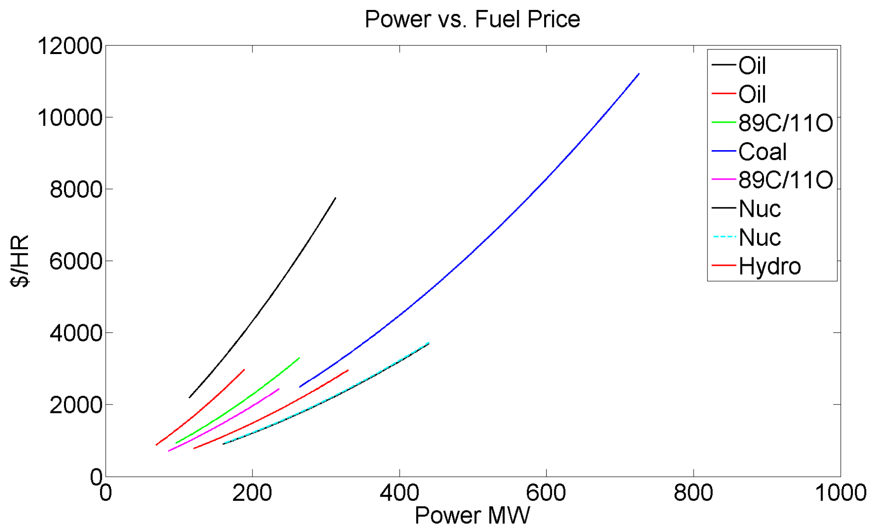

Figure 2.4: Cost function of each generator with maximum and minimum limits implemented

where P_T is the total power:

$$P_T = P_1 + P_2 + ... + P_N \tag{40}$$

P_T is solved initially by summing up the real powers of the loads and adding approximately 5% of the sum of the load powers to account for line losses. Having completed the process the generators with the smallest cost function will typically run at their maximum rated power, while the generators with the largest cost functions are ran at the least amount of power needed to solve load flow.

2.4 Statistics

The statistical portion of probabilistic load flow has had the most updates in modern papers, discussing how to select random data correctly. Among the most important improvements to probabilistic load flow are taking advantage of correlated random variables and selecting data from the multivariate distribution based on this correlation. Correlation is important as wind farms in similar geographical regions may have correlated values as may loads in close proximity to each other.

2.5 Correlation

The correlation coefficient is given by[17]:

$$r = \frac{1}{n-1} \frac{\sum_{i=1}^{n} (y_i - \overline{y})(x_i - \overline{x})}{s_y s_x} \tag{41}$$

$$= \frac{\sum_{i=1}^{n} (y_i - \overline{y})(x_i - \overline{x})}{\sqrt{\sum_{i=1}^{n} \left(x_i^2 - n\overline{x}\right)\left(y_i^2 - n\overline{y}\right)}} \tag{42}$$

where n is the number of data points, x and y are the collected data points, $\overline{x}$ and $\overline{y}$ are the mean values of the collected data, and s_y and s_x are the sample standard deviations. The correlation coefficient is a dimensionless number that lies between -1 and 1. If the correlation coefficient is 1 or -1 then the data has a perfect linear relationship, the closer the coefficient gets to zero, the relationship becomes less linear. A correlation coefficient of zero indicates that a linear relationship between the data does not exist.

2.5.1 Wind and Load Distributions

The chi squared test is a test for the fit of a sample distribution to a particular distribution. The chi squared statistic is given by:

$$\chi^2 = \sum \frac{(Observed - Expected)^2}{Expected} \tag{43}$$

$$= \frac{(O_1 - E_1)^2}{E_1} + \frac{(O_2 - E_2)^2}{E_2} + ... + \frac{(O_k - E_k)^2}{E_k}$$

where k is the number of classes of the data, for example a coin would have 2, and a die would have 6. The number of degrees of freedom is (k-1). The chi squared statistic is the magnitude of the relative error of the function with respect to the expected value. The statistic shows how close one is to the expected value after all the trials. These values come back discrete, but can be well fit with the chi-square distribution which is a special case of the gamma distribution[17]:

$$f = x^{\alpha-1} \frac{e^{-x/\beta}}{\beta^{\alpha}\Gamma(\alpha)} \tag{44}$$

with the parameters $\alpha = k/2$ and $\beta = 2$. If k = 2 the function becomes the exponential distribution. Different distributions can be formed from the chi squared distribution based on the number of constraints c, and degrees of freedom. For example if the number of constraints = 1 the degrees of freedom are (k - 1) and distribution is assumed binomial, if the number of constraints = 2 the degrees of freedom are (k - 2) and the distribution is Poisson, if the number of constraints = 3 the degrees of freedom are (k - 3) and the distribution is normal, lastly if the number of constraints = 4 the degrees of freedom are (k - 4) and the distribution is Weibull [18].

Wind studies have shown that the Weibull distribution best characterizes wind speed data for long periods of time, while wind data for short periods are an unknown distribution still under study [7]. The Weibull distribution pdf is given by

$$\begin{aligned} f(x) &= \frac{k}{\lambda}\left(\frac{x}{\lambda}\right)^{k-1} e^{-(x/\lambda)^k} \quad && for \;\; x \geq 0 \\ f(x) &= 0 && for \;\; x < 0 \end{aligned} \tag{45}$$

where λ is the scale parameter, k is the shape parameter, and constraints are: $\lambda > 0$, $k > 0$, $x \geq 0$, and $0 \leq prob < 1$.Figure 2.5 shows the difference in shape and scale parameters:

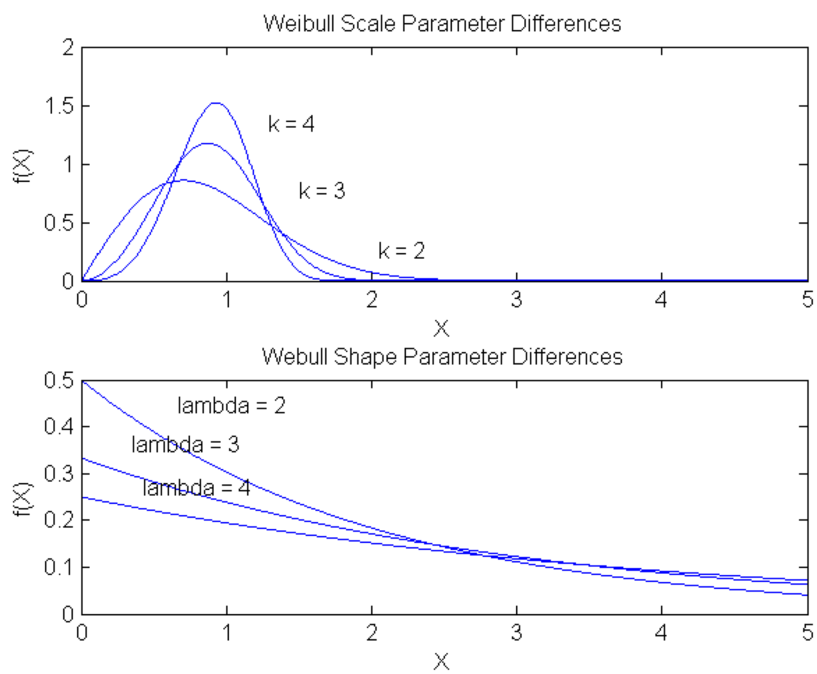

Figure 2.5: Difference between Weibull shape (top) and scale (bottom) parameters

Load distributions can take on multiple forms depending on the data and time-frame selected. For instance choosing weekdays vs weekends, day time vs night time, and different seasons will help create a more narrow distribution and can sometimes appear normal.

2.5.2 Multivariate Distribution

The multivariate distribution is used to randomly select dependent data, and is created when data is obtained from multiple correlated sources. The process is done as follows:

1. Calculate the correlation coefficients between sets of data.
2. Select a random variable from the first set of data.
3. Use the following criteria to create a normal distribution to select the remaining random variables.

$$E(Y|X) = \mu_k + \rho_{1k}\frac{\sigma_k}{\sigma_1}\left(\overline{X} - \mu_1\right) \tag{46}$$

$$Var(Y|X) = \sigma_k^2\left(1 - \rho_{1k}\right) \tag{47}$$

where k is the data set 2, data set 3, and so on, μ is the sample mean, σ is the sample variances, ρ is the correlation between the sets of data, and X is the randomly selected variable. The notation $(Y|X)$ stands for choose Y given X. When randomly selecting correlated wind or load data between two sources, the data selected from the second source should resemble the data randomly chosen from the first source. The process of selecting data from the multivariate distribution after randomly selecting a point from the first distribution and correlating the multiple sets of data is described in detail in [17].

The multivariate distribution is better understood in Figure 2.6 where it is created by randomly selecting a data point from the first distribution, then with the criteria mentioned in equations 2.46 and 2.47 a normal distribution is created from which the remaining random variables are selected.

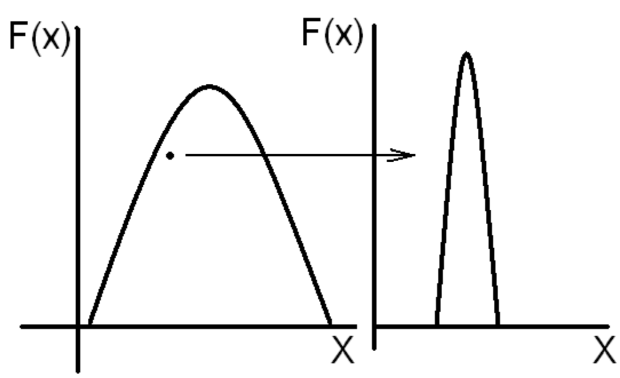

Figure 2.6: Multivariate distribution selection

Note the multivariate distribution can be used for non-normal distributions.

2.6 Probabilistic Load Flow and Generation

Probabilistic load flow and generation is implemented by setting the Wind turbine power output and load data in a uniform distribution to give each data point an equal probability of being selected. The uniform distribution is shown in Figure 2.7 and given by:

$$\begin{aligned} f(x) &= \frac{1}{b-a} \quad for \;\; x \geq 0 \\ f(x) &= 0 \qquad\quad for \;\; x < 0 \end{aligned} \tag{48}$$

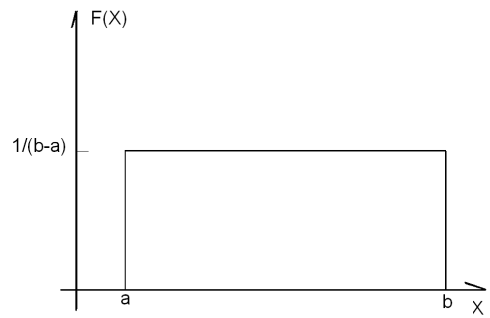

Figure 2.7: Uniform Distribution

The randomly selected variables are then placed in the correct positions of the known vector in the Newton-Raphson method, and calculating deterministic load flow solutions N amount of times. N needs to be a large enough number to not be considered statistically insignificant by the hypothesis test. Results will then also be numerically generated distributions that result from N solutions.

2.6.1 Parallel Computing

The super computer at New Mexico Tech, Exemplar, was used with MATLAB's parallel computing and compilers toolbox. The super computer consists of 22 nodes, where each node contains 2 processors and each processor is composed of 4 cores. Each load flow solution takes approximately 3 seconds to compute. There are 10,000 runs per scenario. Each scenario would take approximately 30,000 seconds $\approx$ 8.33 hours to finish on a local computer in serial. On the super computer the computation time is roughly divided by the number of cores in use (number of nodes (4) * processors per node used(2)*cores per processor(4)) and results return in approximately 0.260 hours or 15.6 minutes. If the super computer was fully utilized (permission to use all 22 nodes) the amount of time taken to compute 10,000 runs would take approximately 3 minutes.

3 Method

3.1 Data Collection

3.1.1 Wind Data

Multiple sets of wind speed data were located off the coast of California and downloaded from National Renewable Energy Laboratory (NREL) website (http://www.nrel.gov). The data for each site was collected for three years, between 2004-2006 at ten minute intervals (157680 points total). The annual average wind speed is placed into one of ten wind speed categories based on its magnitude. Category 7 wind speed data was chosen to account for the wind speeds of the island power grid in study. Figure 3.1 displays a California wind speed site histogram and corresponding best fit representation of a Weibull distribution overlay which illustrate how well the Weibull distribution fits the real data. Figure 3.2 displays the wind speed vs. time plot for the same data. The data downloaded from the NREL website is placed in the following format for ease and readability in MATLAB.

Year	Month	Day	Hour	Minute	Wind Speed(m/s)
2004	7	8	23	30	17.96
2004	7	8	23	40	17.94
2004	7	8	23	50	17.9
2004	7	9	0	0	17.9
2004	7	9	0	10	17.9
2004	7	9	0	20	17.89
2004	7	9	0	30	17.86
2004	7	9	0	40	17.86

Table 3.1: Example of the wind speed data format

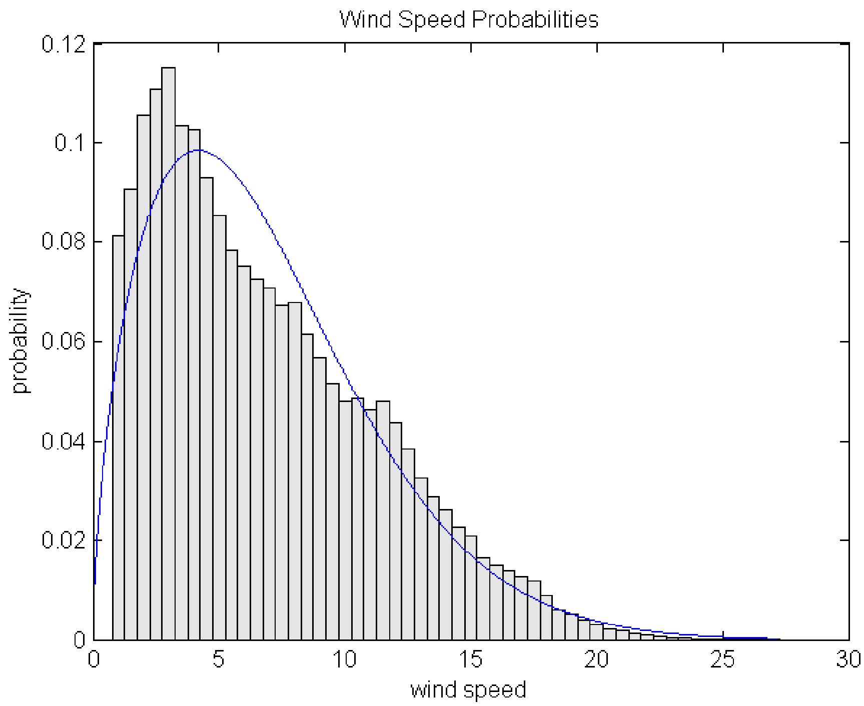

Figure 3.1: Wind speed data histogram with Weibull distribution overlay

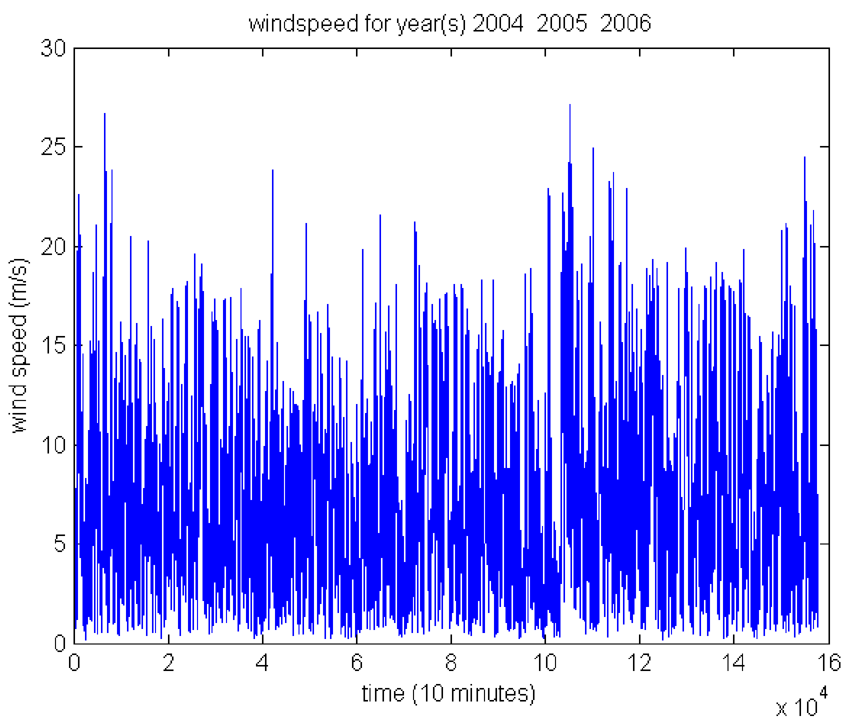

Figure 3.2: Wind speed vs time plot

3.1.2 Load Data

A local electric co-op provided load data from a substation for two small southern New Mexico towns with thirty minute interval measurements on dates raging from 8/30/2009 to 9/1/2010 (17520 points total). The real and reactive powers, and voltages were measured for each phase. To convert to a one-line representation the average of the voltages and the sum of the real and reactive powers was computed. Plots of real and reactive power vs time are shown in Figure 3.3 and 3.4. Histograms of the same data are displayed in Figure 3.5 and 3.6. The data was placed in the format shown in Table 3.2.

Year	Month	Day	Hour	Minute	V1	V2	V3	AVG(V's)...
2009	8	30	0	0	14950	14930	14899	14926.3...
2009	8	30	0	30	15007	14995	14976	14992.6...
2009	8	30	1	0	15026	15021	14994	15013.6...
2009	8	30	1	30	15006	14971	14873	14950...
2009	8	30	2	0	15047	15013	14921	14993.6...
2009	8	30	2	30	14971	15035	14930	14978.6...

...P1	P2	P3	$\sum Ps$	Q1	Q2	Q3	$\sum Qs$
...544	505	677	1726	480	580	536	1596
...536	476	646	1658	480	580	536	1596
...505	466	646	1617	480	580	536	1596
...503	464	600	1567	482	596	546	1624
...511	466	615	1592	478	592	549	1619
...493	457	650	1600	476	594	546	1616

Table 3.2: Example of the load data format

3.2 Time Intervals For Load Selection

Taking only weekend or weekday, daytime or nighttime, upper or lower, and individual monthly data will create narrower distributions to select data from, and therefore a more accurate random variable selection; refer to Figures 3.8 through 3.14. Notice in Figure 3.10 through 3.14 that proper time selections will separate the upper and lower portions of the full time histogram. For the upper and lower load time selection it is helpful to look at the entire season or month of load data and histograms to determine the appropriate time of day that certain thresholds for separation exist, refer to Figures 3.8 and 3.9. Selecting a season, subtracting weekends and plotting the times that the real load power is above and below this threshold creates desirable time intervals from which data is chosen. For example, weekdays in the spring have the following upper and lower threshold values, $\geq$ 6500MW and $\leq$ 6000MW respectively with a relatively small 500MW cross over. Selecting these upper and lower load thresholds yield the time intervals shown in Figure 3.7, which can be used to randomly select data.

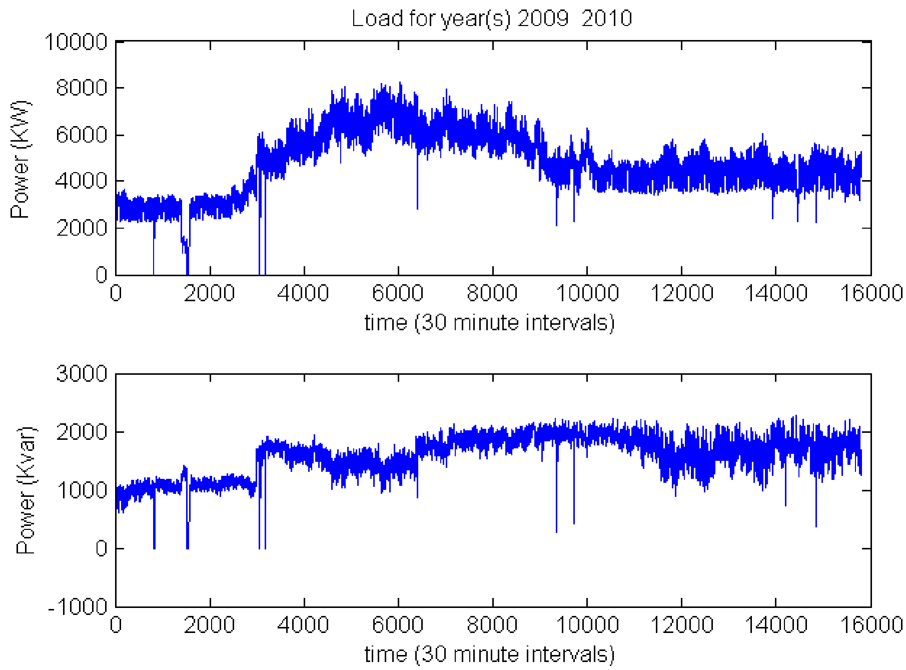

Figure 3.3: Active and reactive load powers vs time for Town 1

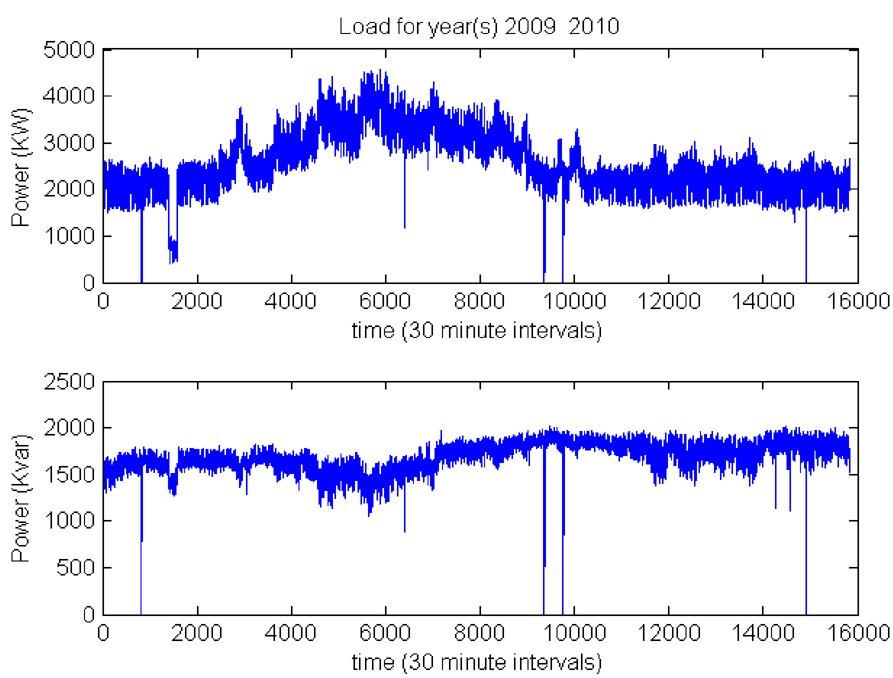

Figure 3.4: Active and reactive load powers vs time for Town 2

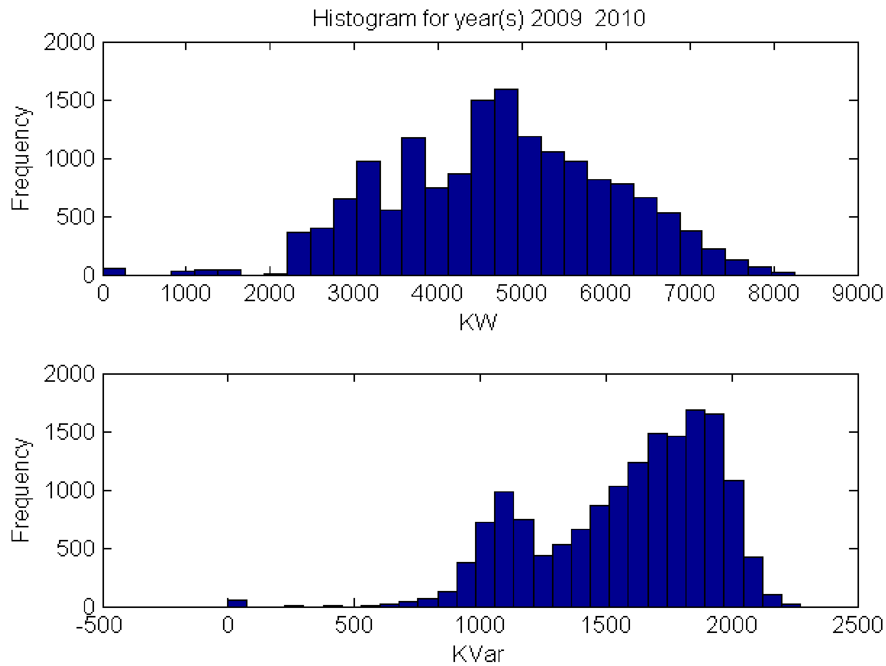

Figure 3.5: Histograms of load active and reactive power for Town 1

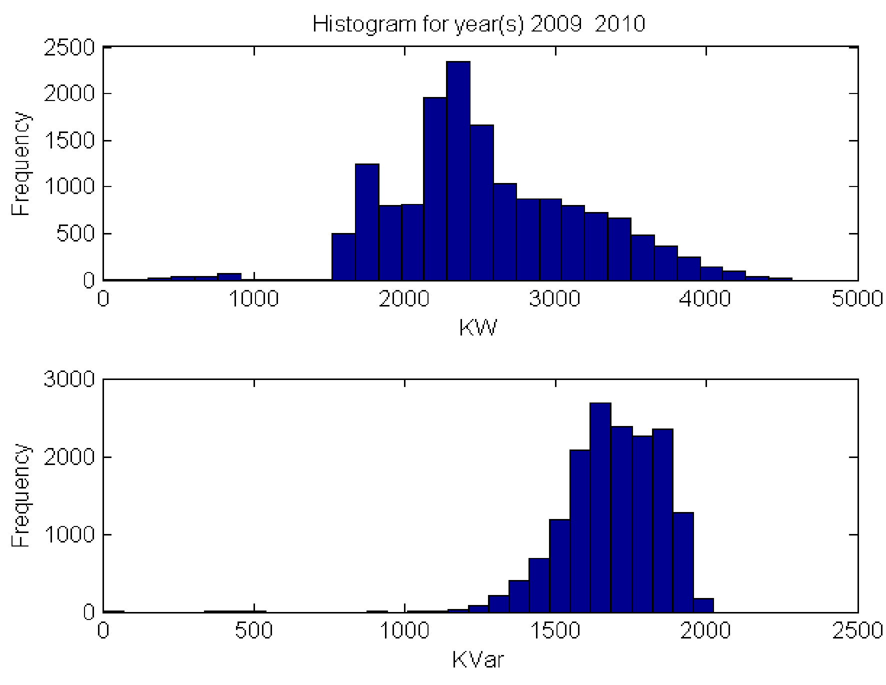

Figure 3.6: Histograms of load active and reactive power for Town 2

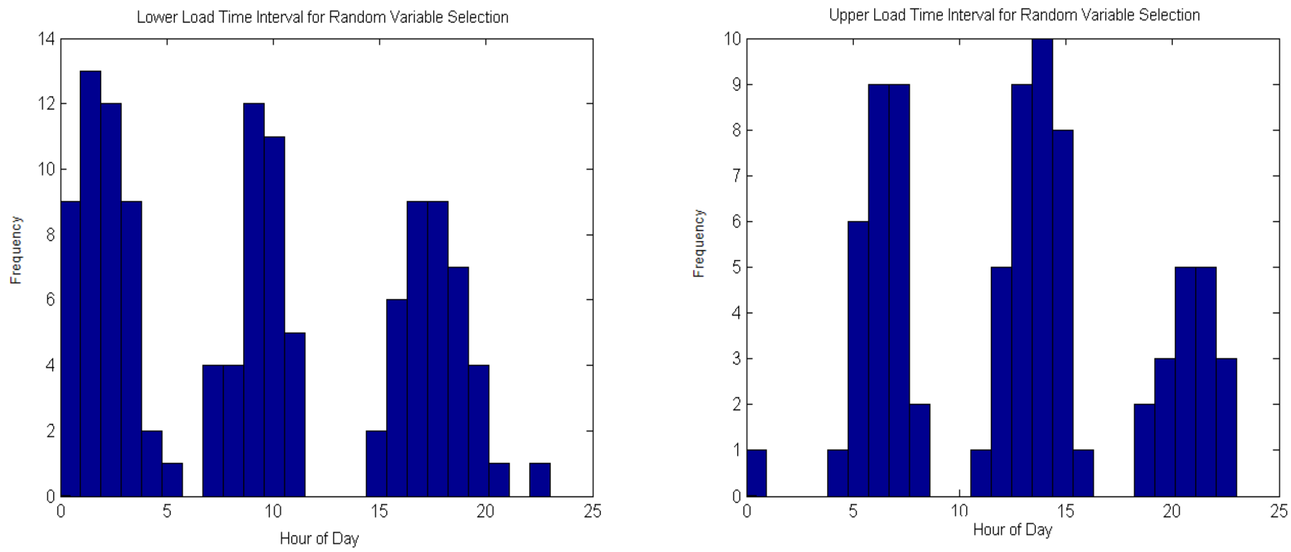

Figure 3.7: Time histograms for P≤ 6000MW (top) and P≥ 6500MW (bottom) threshold

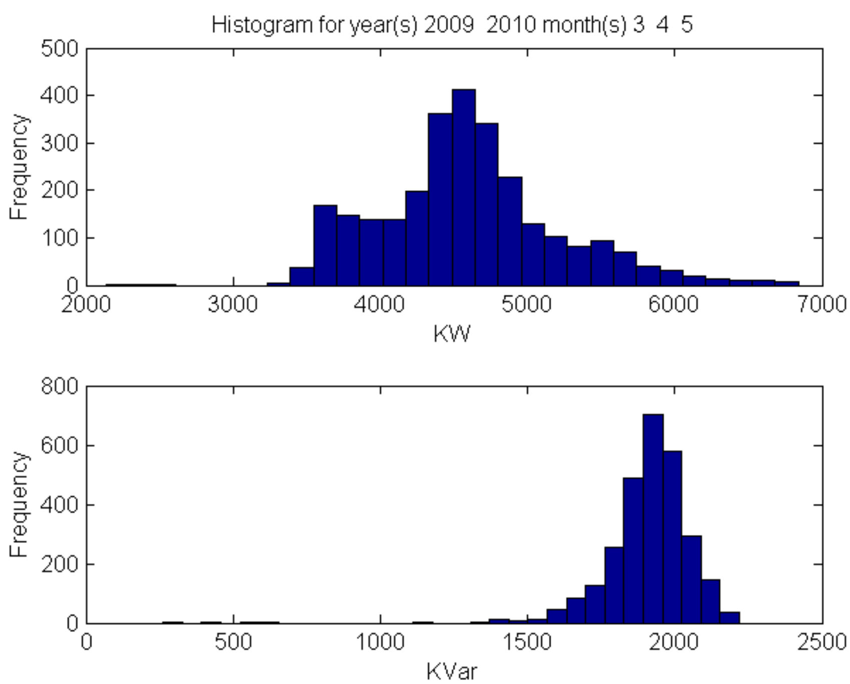

Figure 3.8: Spring seasonal real and reactive load histograms

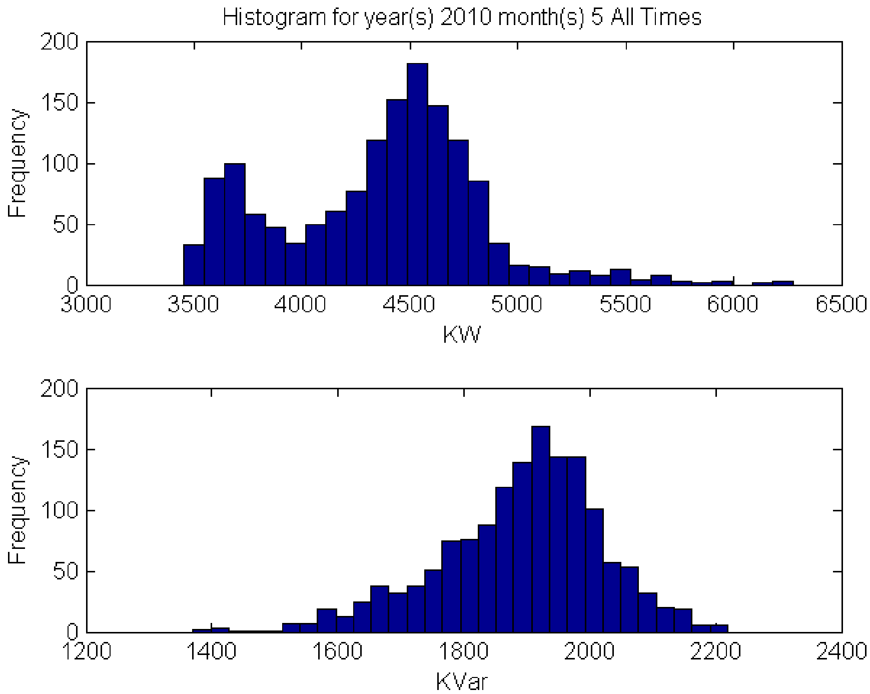

Figure 3.9: May real and reactive load histograms

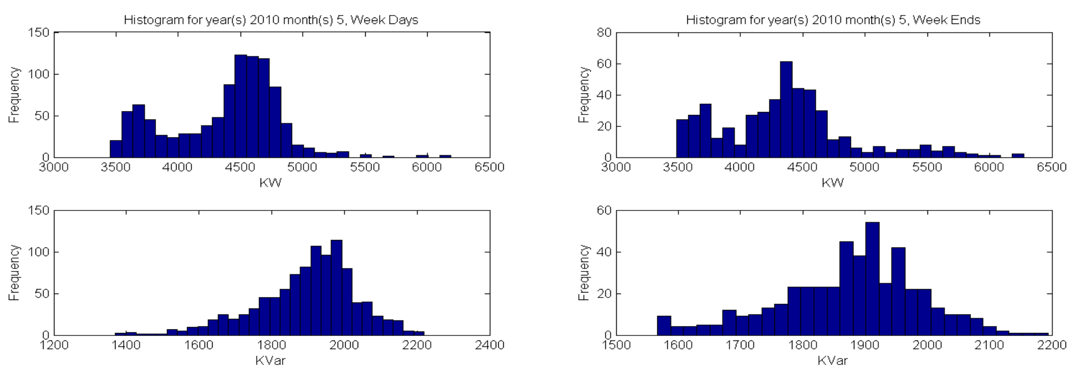

Figure 3.10: Weekday (left) and weekend (right) real and reactive load histograms for May

3.2.1 Grid Data and Parameters

The IEEE 24-bus test systems described in section 2.4 will be utilized for the probabilistic load flow based study to follow. The probabilistic load flow algorithm developed does not allow generators and loads connected at one bus due to each corresponding to a different bus type (PV vs PQ). There are a couple methods for addressing this problem. The first method is to take the difference between the real and reactive generator and load powers and denote the bus either a generator bus if the difference is positive or a load bus if

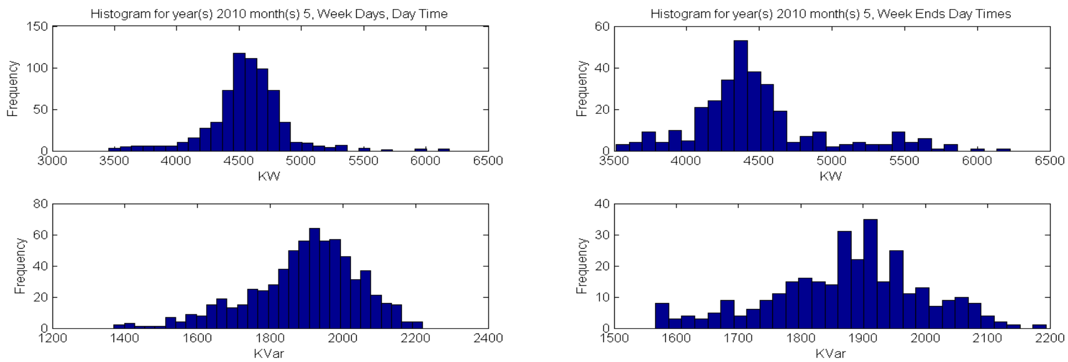

Figure 3.11: Weekday (left) and weekend (right) day time real and reactive load histograms for May

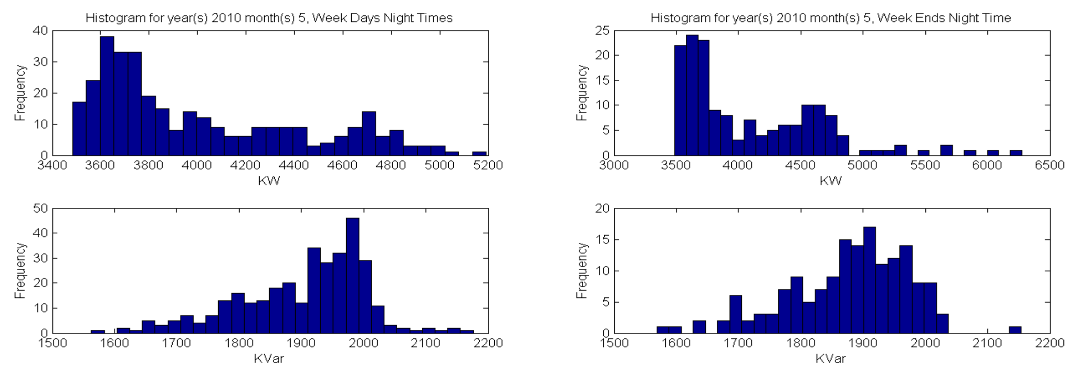

Figure 3.12: Weekday (left) and weekend (right) night time real and reactive load histograms for May

the difference is negative. A second method involves creating additional buses, where the generators are separated from the loads. This posses more problems with having new line and bus data, however using a low connecting impedance between the two buses, on the order of a magnitude or less than the original line parameters will keep the system close to its original form. The second method was chosen for its more accurate representation of a real system. Where the first method removes the total number of loads and generators, and assumes that the generator and load connected at the bus are taken care of solely by the remaining device instead of the grid as a whole. The new line parameters are:

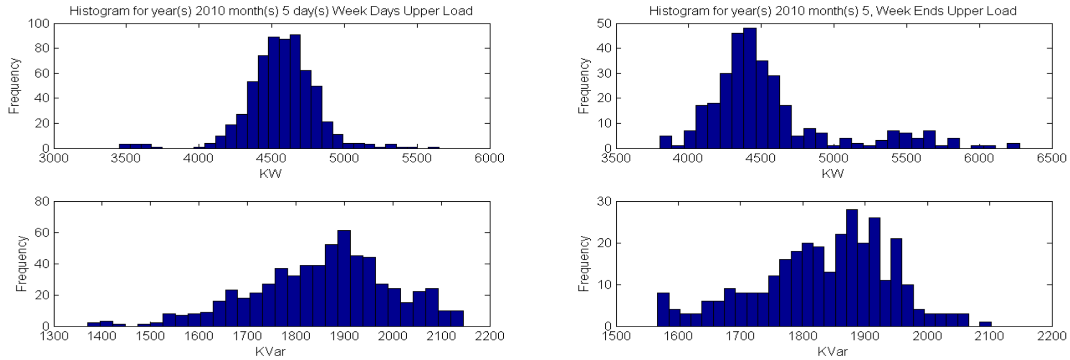

Figure 3.13: Weekday (left) and weekend (right) upper load time interval real and reactive load histograms for May

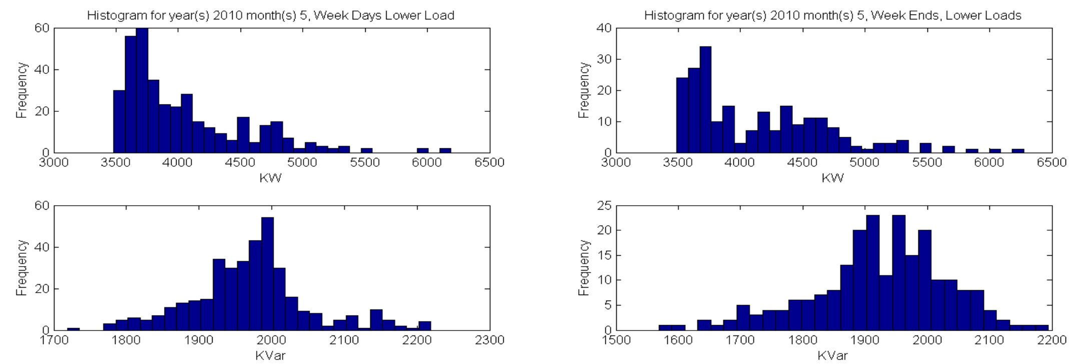

Figure 3.14: Weekday (left) and weekend (right) lower load time interval real and reactive load histograms for May

Bus From	Bus To	R	X	G	B
1	25	0.0001	0.001	0	0
2	26	0.0001	0.001	0	0
7	27	0.0001	0.001	0	0
13	28	0.0001	0.001	0	0
14	29	0.0001	0.001	0	0
15	30	0.0001	0.001	0	0
16	31	0.0001	0.001	0	0

Table 3.3: IEEE 24-bus system line data added to separate generators and loads

3.3 Interpolating Wind Data

The goal of this process is to create a polynomial that resembles the manufactures power curve that relates wind speed (input) to power produced (output). The GE 2.5xl wind turbine full converter model was chosen due to its recent popularity[19]. This model accounts for approximately 80% of the total wind tubines sold in 2010. Its popularity results from advances in control and fault ride through capability[11]. The power curve for the GE 2.5xl is shown in Figure 3.15.

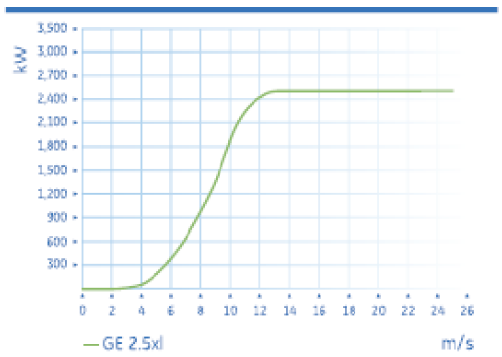

Figure 3.15: GE 2.5xl wind turbine power curve

In order to interpolate data, a set of data points for the power curve was gathered from the data sheet.

Ws	1	2.4	3.57	4.17	4.77	5.36	5.96	6.56	7.75	8.35	8.94	10.13	12.6	13.5
P	0	0	0.043	0.21	0.38	0.55	0.72	0.88	1.22	1.39	1.55	1.89	2.5	2.5

Where W_s vs $P(W_s)$ is plotted, and the cubic spline interpolation method is performed. The coefficients found between selected points in the non linear region from this method are:

$$a = \text{-0.0004},\ b = \text{-0.0001},\ c = 0.2894, \text{ and } d = \text{-.09813}$$

where the polynomial has the form $aW_s^3 + bW_s^2 + cW_s + d$. Having P_3 as the most dominant weighted factor, shows that the curve is nearly linear. The piecewise polynomial created from the interpolation is displayed on top of the data in Figure 3.16.

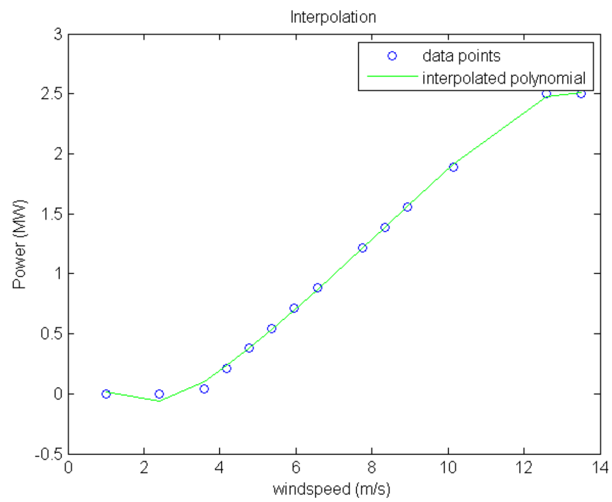

Figure 3.16: Interpolated polynomial for wind speed vs wind turbine power output data points

The absolute and relative error ($|p - p^*|$ and $|p - p^*|/|p|$) between the data and approximation is displayed in Table 3.4, where p is the gathered data point and p^* is the approximated point. Notice that the relative error is large for the third and fourth point, however the

Data Points	Polynomial Points	Absolute Error	Relative Error	Relative Error %
0	0.0146	0.0146	na	na
0	-0.0640	0.0640	na	na
0.0430	0.1042	0.0612	1.4231	142.31%
0.2110	0.2324	0.0214	0.1015	10.15%
0.3790	0.3788	0.0002	0.0004	0.04%
0.5470	0.5352	0.0118	0.0216	2.16%
0.7150	0.6997	0.0153	0.0213	2.13%
0.8830	0.8670	0.0160	0.0181	1.81%
1.2190	1.2118	0.0072	0.0059	0.59%
1.3870	1.3865	0.0005	0.0003	0.03%
1.5550	1.5625	0.0075	0.0048	0.48%
1.8910	1.9134	0.0224	0.0119	1.19%
2.5000	2.4753	0.0247	0.0099	0.99%
2.5000	2.5124	0.0124	0.0049	0.49%

Table 3.4: Absolute and relative error

difference between the points, shown in the absolute error, are on the same order as the rest of the absolute error calculations. Also the relative error is less than 2.2% for the rest of the data points, in fact most of the data points have a relative error less than 1%.

The next step is to turn the wind speed data into real power data based on the wind turbines cut in speed, cut out speed, rated capacity speeds, and the newly created polynomial $P(W_s)$ speeds. Cut in and cut out speeds both deliver zero output, while at the rated capacity the maximum output is 2.5 MW. The interpolated polynomial has an output based on the curve formed from the nonlinear curve. The criteria for the GE 2.5xl wind turbine are:

- below cut in speed: < 3.5 m/s
- cut out speed: ≥ 25 m/s
- rated capacity/optimal speed: ≥ 12.5 m/s and < 25 m/s
- polynomial related speeds: > 3.5 m/s and < 12.5 m/s

The entire site's data is plotted according to the above criteria and is shown in Figure 3.17. Figure 3.18 displays a histogram of the real output power and is the basis of selecting random data for the first simulated wind farm. Selecting data from the next wind farm in sequence is described in more detail back in section 2.4.3, Multivariate Distribution.

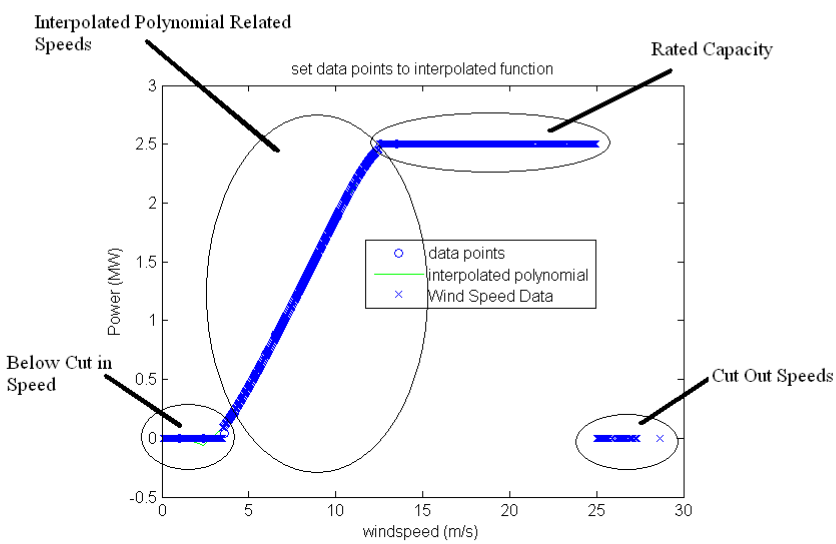

Figure 3.17: Final wind turbine power vs. wind speed power curve

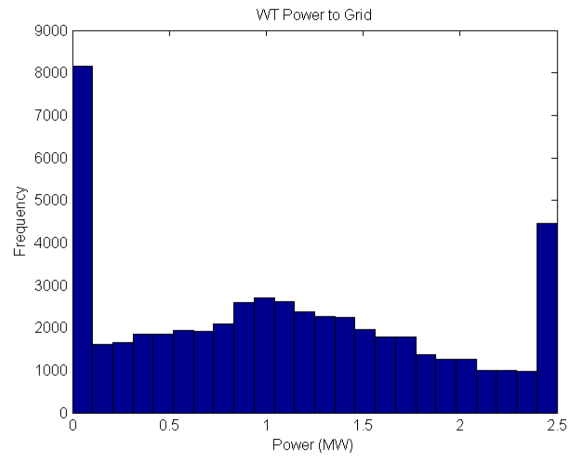

Figure 3.18: Histogram of real power from wind turbine at wind speeds taken from data

3.4 Statistical Calculations

The wind data was selected to have three highly correlated sites and one site less correlated. The correlation matrix between the wind sites for the entire data is:

$$\begin{bmatrix} 1.0000 & 0.9971 & 0.9957 & 0.6825 \\ 0.9971 & 1.0000 & 0.9984 & 0.6828 \\ 0.9957 & 0.9984 & 1.0000 & 0.6870 \\ 0.6825 & 0.6828 & 0.6870 & 1.0000 \end{bmatrix}$$

where the matrix is symmetrical and its row (i) and column (j) describes the correlation between site (i) and (j). The diagonal element is the correlation between one site and its self.

The correlation matrix between the load sites for the entire data is:

$$\begin{bmatrix} 1.0000 & 0.6283 \\ 0.6283 & 1.0000 \end{bmatrix}$$

The mean and standard deviations in p.u. for the wind and load power data is shown in Table 3.5. The p.u. quantities were computed via the method described in section 2.2

3.5 GE Full Converter Wind Turbine

The full converter wind turbine is similar to the DFIG wind turbine model where both have extensive rotor to stator side converter controls. The flux dynamics can be eliminated due to the rapid response from the controls [11]. The DFIG and full converter dynamic models are very similar, however the full converter is completely disconnected from the grid

Data Set	Mean (P.U)	Standard Deviation (P.U)
wind data 1	1.3608	1.2752
wind data 2	1.3747	1.3130
wind data 3	1.3593	1.3083
wind data 4	1.4390	1.1123
load data 1(P)	1.8972	0.5274
load data 1(Q)	0.1981	0.0434
load data 2(P)	1.0713	0.2676
load data 2(Q)	0.2113	0.0203

Table 3.5: Mean and standard deviations of wind and load data sets

through the power converter electronics or network frequency converter, where as the DFIG has a voltage source converter connected to a set of slip rings. One of the slip rings is connected to the stator side and the other is connected to the rotor side. Thus the DFIG remains partially connected to the grid [10].

3.5.1 Controls

Typical wind turbines have two types of control, power factor and voltage, that can be interchanged. Wind turbine connecting buses can take on two forms depending on what kind of control is being used. The bus is considered a negative PQ bus if power factor control is being used, or a PV bus if voltage control is being used. Power factor control is set up assuming a constant power factor (PF) of 0.95.

$$PF = cos(\theta) = 0.95 \tag{49}$$

Where θ is the difference between the bus voltage and injected current angles. solving for θ and plugging into the relation:

$$\frac{Q}{P} = tan(\theta) \tag{50}$$

gives Q as a known quantity. This method can be understood with the power triangle shown in Figure 3.19.

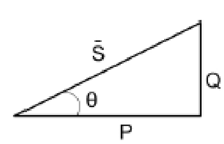

Figure 3.19: Power triangle

where S is the complex power, P is the real power, and Q is the reactive power. Voltage control is done simply by setting the voltage at the connecting bus (V) to a constant 1 p.u.

Figure 3.20: Maximum reactive power allowed from a full converter wind turbine

3.5.2 Reactive Power Maximum and Minimum Limits

DFIG and full converter wind turbines are capable of delivering reactive power when there is no presence of wind or real power output and is determined by the bus voltage and injected bus current limitations on the stator and rotor side of the wind turbine [10]. However maximum and minimum reactive power limits exist for both models. For the GE 2.5 xl the maximum and minimum reactive power is a percentage of the maximum real power, 0.4 and -0.4 respectively [11], and is shown in Figure 3.20 [20]. The wind turbines are initially set to have voltage control making the connecting bus a PV bus. If the reactive power becomes greater than the maximum tolerance, the reactive power is set to the maximum limit and converted to a PQ bus. Deterministic load flow is ran again with the new configuration, and solves the new unknown voltages and reactive powers until all wind turbine generator buses are within the tolerable reactive power range.

3.6 Scenarios

Ten thousand load flow simulations were performed for eleven different scenarios on the modified IEEE 24-bus system consisting of two new wind farms replacing two of the generators. The average of the wind farms real power is set to the amount of power it is replacing. The total amount of wind power penetration taken at the wind speeds average is 10.7%. The grid recieves approximately 20% renewable penetrations at the maximum wind power output. The modified system is displayed in Figure 3.21.

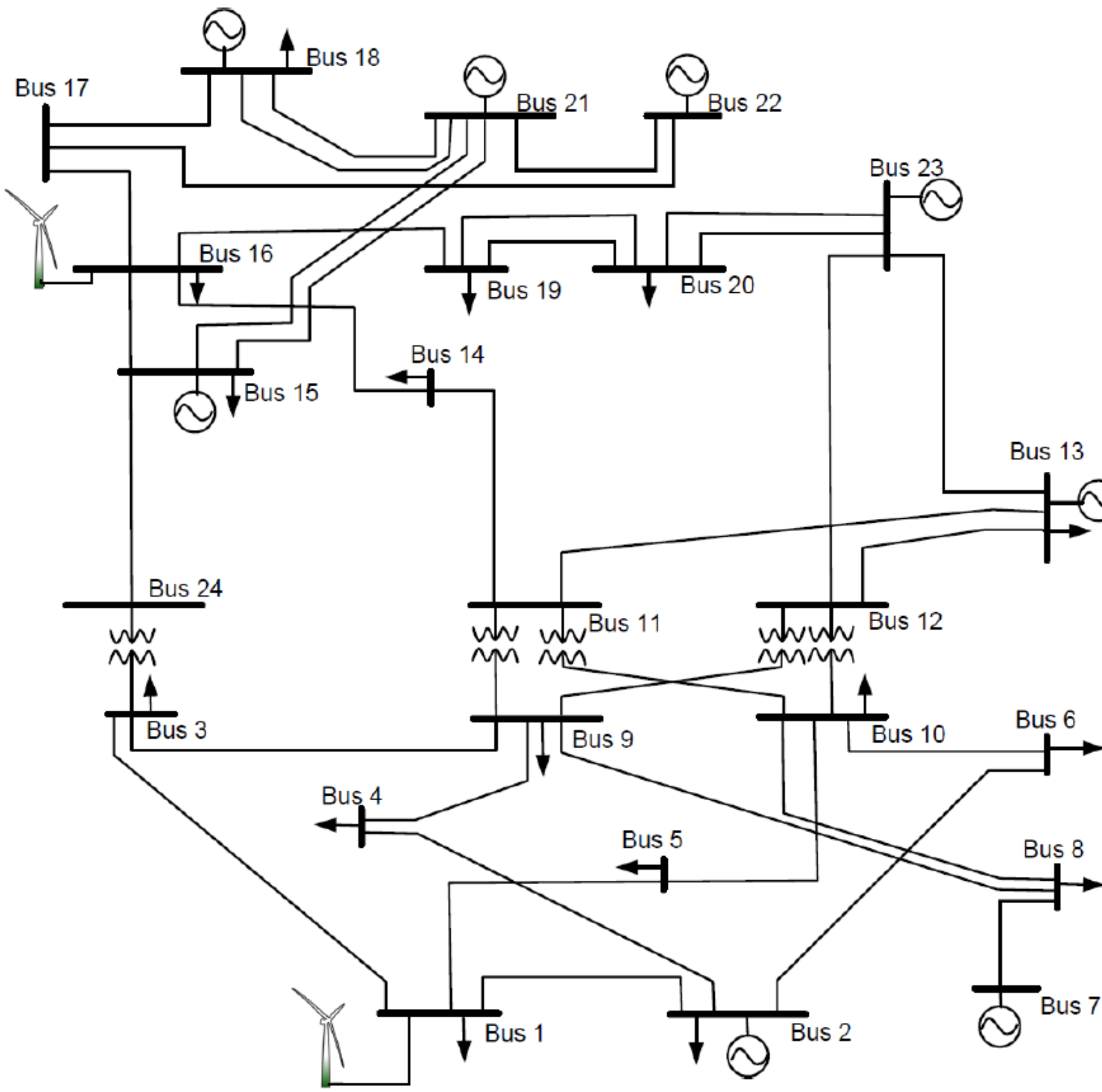

Figure 3.21: Maximum reactive power allowed from a full converter wind turbine

Each scenario is distinguished by the time of day the random variables are selected. Each scenario takes place in the month of November and scenarios include:

UWD	upper load interval weekday
UWE	upper load interval weekend
LWD	lower load interval weekday
LWE	lower load interval weekend
DWD	daytime load weekday
DWE	daytime load weekend
NWD	nighttime load weekday
NWE	nighttime load weekend
AWD	all time load weekday
AWE	all time load weekend
AAT	all time load all days

Table 3.6: Time Interval Scenarios

Since the data is enormous only weekday values will be displayed for load flow and economic dispatch results. The upper and lower intervals are selected containing the upper and lower load threshold times for the weekdays of November. The weekday upper load threshold hours are between 12:00 midnight to 5:59 A.M. and 10:00 A.M. to 5:59 P.M. The lower load threshold hours are between 5:00 A.M. to 10:59 A.M. and 5:00 P.M. to 11:59 P.M. The day time hour selection consist of the time the load starts increasing in the morning, 5:00 A.M. to the time the load starts decreasing at night, 8:59 P.M, leaving the night time hours between 9:00 P.M. to 4:59 A.M.

3.7 Method Overview

The following two figures reiterate the process of splitting up the load data, and how the inputs are chosen for the system. In Figure 3.22 a sample of one weekday's power vs. time is plotted at the top to illustrate the selection of the upper and lower load sections. The histogram on the left displays the weekday powers for the entire month. The top and bottom histograms display the above and below selected threshold powers, respectively. The histogram on the right shows the intervals of time that the above and below selected threshold loads exist. These are the times that the load and wind power random variables are selected for the upper and lower scenarios.

Figure 3.23 is a summary of the entire process. A random variable is selected from one of the scenarios for the first load. Then based on that random variable, the correlation between data sets for loads, and the criteria mentioned for the multivariate distribution, a new distribution is created from which the remaining loads are chosen. The random variable for the first wind farm power input is selected at the same time interval as the load. The multivariate distribution is used again to select the remaining wind farm powers. The traditional generator's inputs adjust based on the inputs from the loads and wind farm power according to their cost functions from economic dispatch.

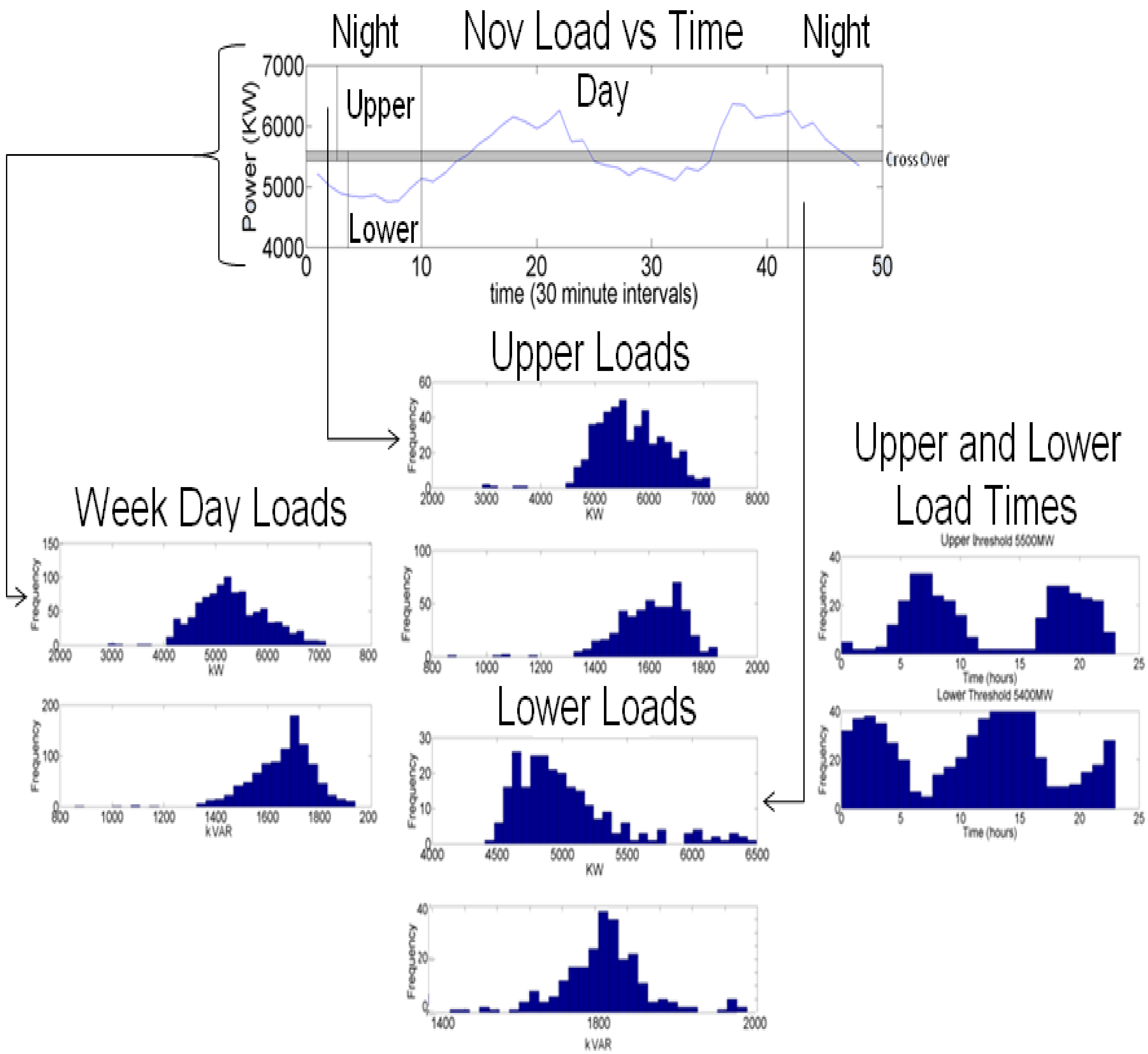

Figure 3.22: Summary of selecting upper and lower load sections

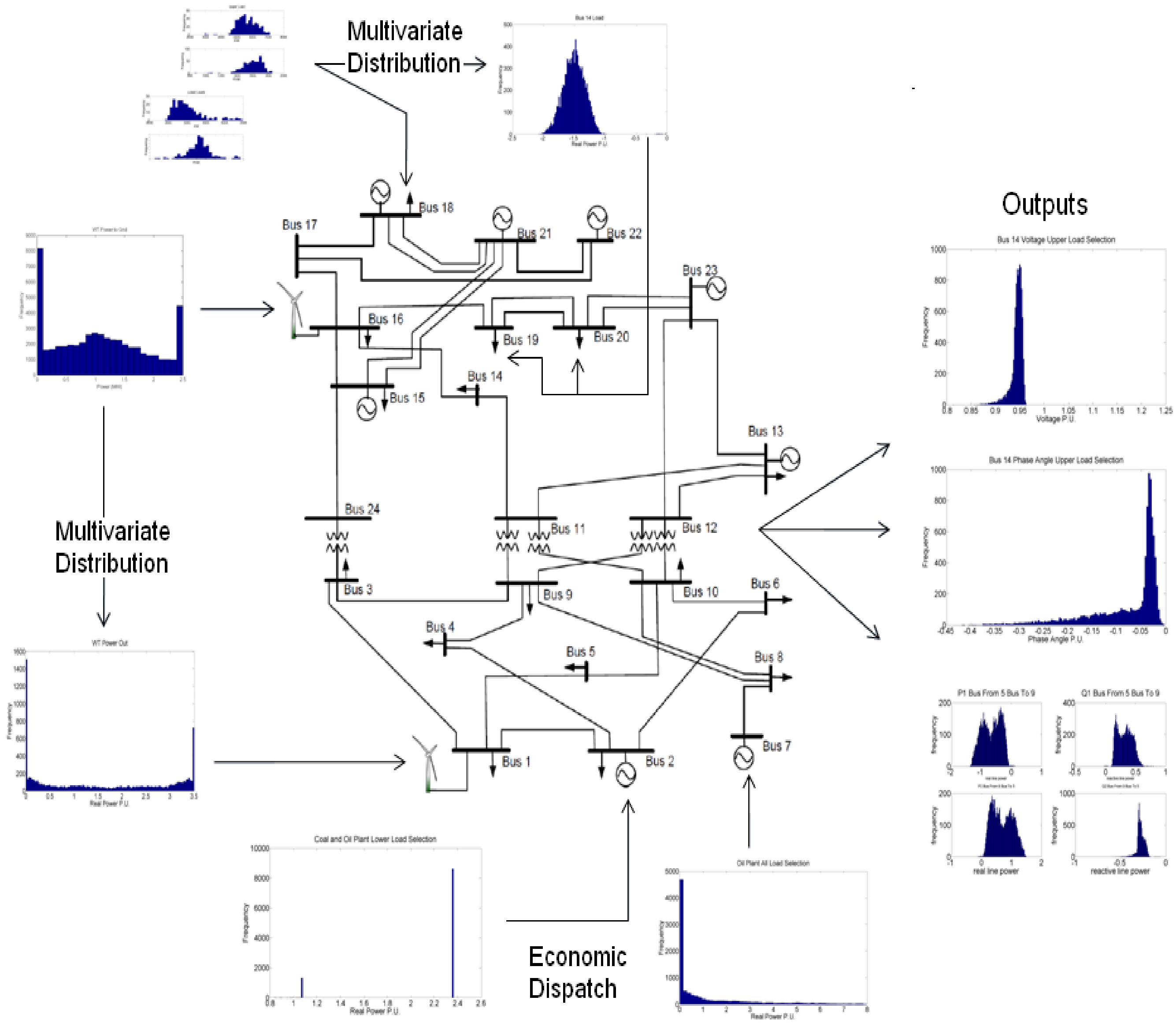

Figure 3.23: Summary of entire process

4 Results

4.1 Load-Flow

This section displays statistical results using basic load flow techniques without the use of wind turbine reactive power control. For this study the data was selected on the weekdays of November 2009. Table 4.1 displays the means and standard deviations of the voltages at selected buses for weekday scenarios. The percentage of voltages that fall above or below the NERC standards, 1.05 p.u. and 0.92 p.u., respectively, are displayed in the row labeled NERC. The last 4 rows include the statistics of the failed to converge runs via the Newton-Raphson method, and the correlation between real and reactive load data between town 1 and town 2. The average values and standard deviations are also calculated, for line powers on all week day scenarios for the line connecting bus 5 to bus 9 and shown in Table 4.2. P1 and P2 are the real powers from bus 5 to 9 and bus 9 to 5, respectively, Q1 and Q2 are the reactive powers from bus 5 to 9, and bus 9 to 5, respectively, and S is the apparent power.

Table 4.1 reveals that the lower weekday (LWD) potion of the load distributions has on average the smallest variance, lowest NERC violations, and second smallest failed convergence rate, where on average the largest variance is found in the upper weekday (UWD) portion of the load distribution. Daytime weekday (DWD) load, nighttime weekday (NWD) load, and all weekday (AWD) load distributions appear in between UWD and LWD. Phase angles and line powers have similar results. Breaking up the load distribution into upper and lower portions proves to give a better variance for one of the two scenarios. Taking the average of the combination of UWD and LWD scenarios, and DWD and NWD scenarios and comparing to the AWD scenario reveal that the UWD and LWD have a smaller number of NERC violations than the combination of DWD and NWD, and the full AWD scenarios. However, the greatest number of failed convergences occurs for the combination of UWD, and LWD scenarios. Figures 4.1 through 4.6 are histograms of voltages and phase angles of one selected bus, using UWD, LWD, and AWD scenarios. Notice in Figures 4.1 through 4.3 there are cases that the voltages fall below the NERC standards where decisions can be made on how to fix the problem. Figure 4.7 through 4.9 are the slack bus fluctuations for UWE, LWD, and AWD scenarios. Notice that basic load flow methods predict that the generator absorbs generation a percentage of the time, as well as has to supply above realistic amounts of power in order to solve the power balance equations. Table 4.2 reveals that the LWD scenario has the second smallest standard deviation and mean, and the UWD scenario has the greatest variance and mean. Figure 4.9 through 4.11 are the line power histograms.

	Scenario	LWD	UWD	DWD	NWD	AWD	AAD
Bus 6	σ^2	0.023	0.031	0.026	0.022	0.025	0.024
	μ	1.025	1.012	1.004	1.007	1.005	1.003
	NERC	2%	2%	2%	1%	2%	1%
Bus 9	σ^2	0.021	0.028	0.025	0.021	0.024	0.022
	μ	0.945	0.933	0.928	0.931	0.929	0.927
	NERC	11%	22%	32%	29%	32%	34%
Bus 14	σ^2	0.012	0.017	0.014	0.012	0.014	0.013
	μ	0.963	0.955	0.949	0.951	0.950	0.949
	NERC	1%	4%	7%	4%	6%	5%
	#Failed	19	210	80	1	27	19
	%Failed	0.19%	1.55%	0.8%	0.01%	0.27%	0.19%
	ρ_P	0.804	0.658	0.668	0.936	0.749	0.796
	ρ_Q	0.515	0.420	0.435	0.752	0.508	0.536

Table 4.1: November weekday voltages and failed runs statistics at selected buses

scenario		μ	σ^2	scenario		μ	σ^2
LWD	P1	-0.398	0.207	NWD	P1	-0.398	0.212
	Q1	0.189	0.123		Q1	0.208	0.119
	P2	-0.411	0.218		P2	-0.412	0.222
	Q2	-0.221	0.075		Q2	-0.236	0.075
	S	0.445	0.232		S	0.457	0.228
UWD	P1	-0.553	0.261	AWD	P1	-0.418	0.213
	Q1	0.277	0.191		Q1	0.222	0.133
	P2	-0.578	0.280		P2	-0.433	0.226
	Q2	-0.265	0.158		Q2	-0.244	0.077
	S	0.641	0.277		S	0.477	0.244
DWD	P1	-0.428	0.230	AAT	P1	-0.442	0.206
	Q1	0.228	0.190		Q1	0.234	0.122
	P2	-0.444	0.245		P2	-0.458	0.217
	Q2	-0.244	0.152		Q2	-0.252	0.073
	S	0.503	0.266		S	0.508	0.221

Table 4.2: November sample line powers for each scenario connecting bus 5 to 9

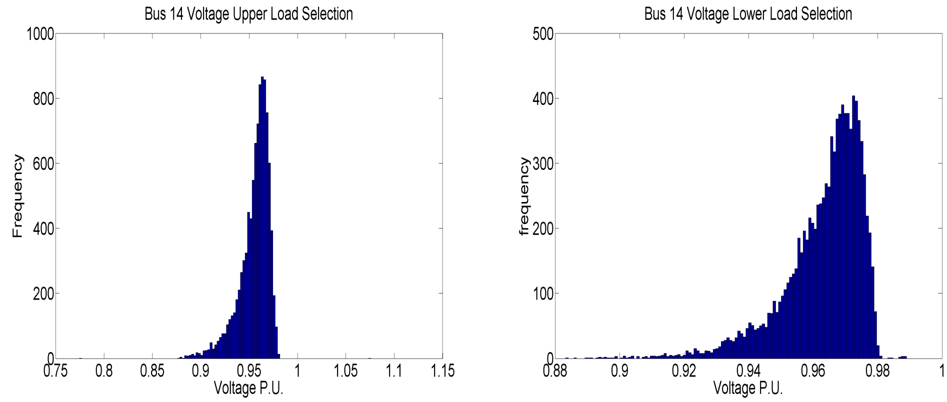

Figure 4.1: Bus 14 voltage histograms using upper (left) and lower (right) portions of load distributions

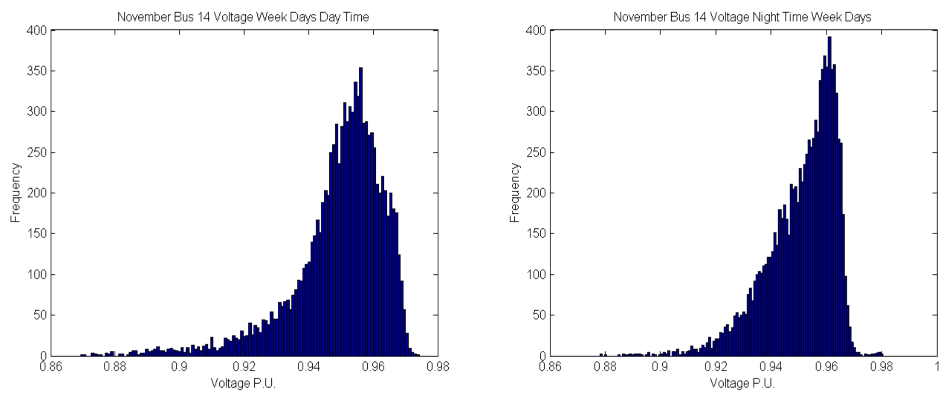

Figure 4.2: Bus 14 voltage histograms using daytime (left) and nighttime (right) load distributions

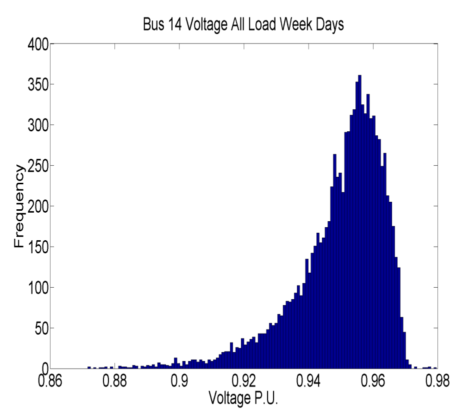

Figure 4.3: Bus 14 voltage histogram using the full load distribution

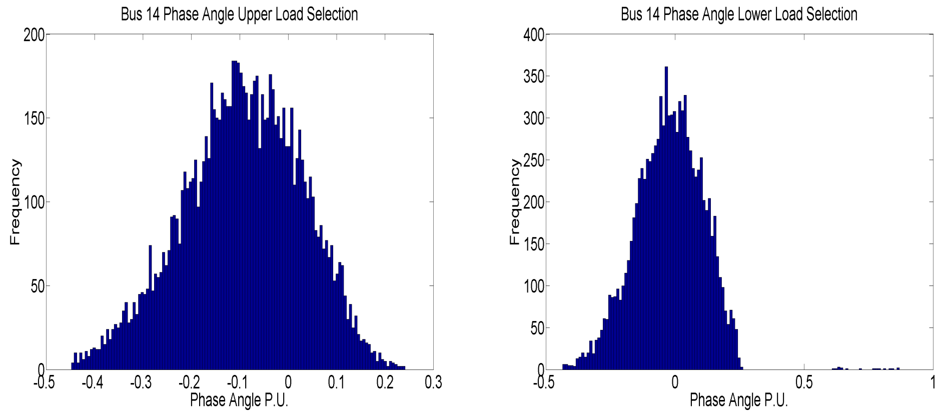

Figure 4.4: Bus 14 phase angle histograms using upper (left) and lower (right) portions of load distribution

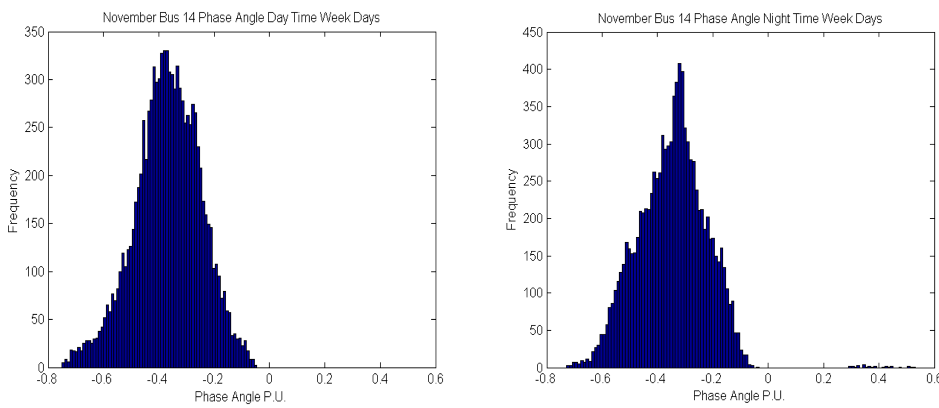

Figure 4.5: Bus 14 phase angle histograms using daytime and nighttime load distributions

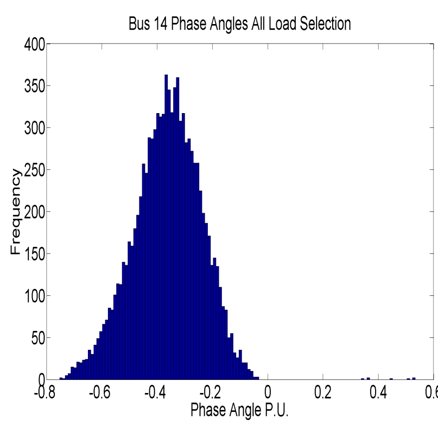

Figure 4.6: Bus 14 phase angle histogram using the full load distribution

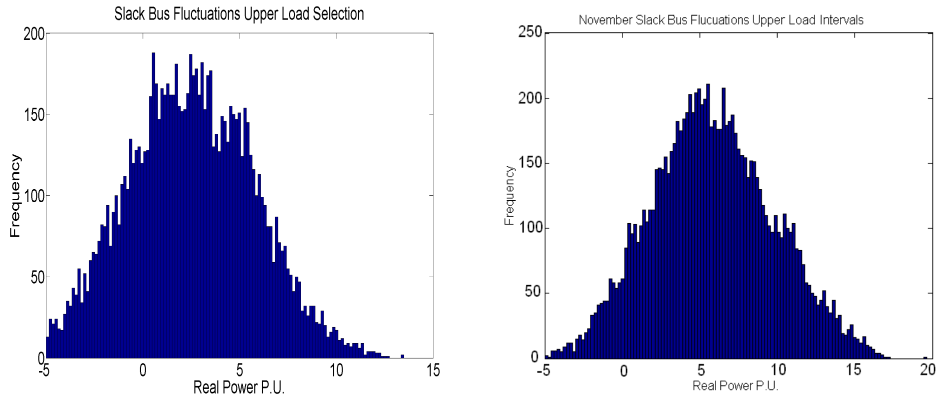

Figure 4.7: Slack bus fluctuation histograms using upper (left) and lower (right) portions of load distribution

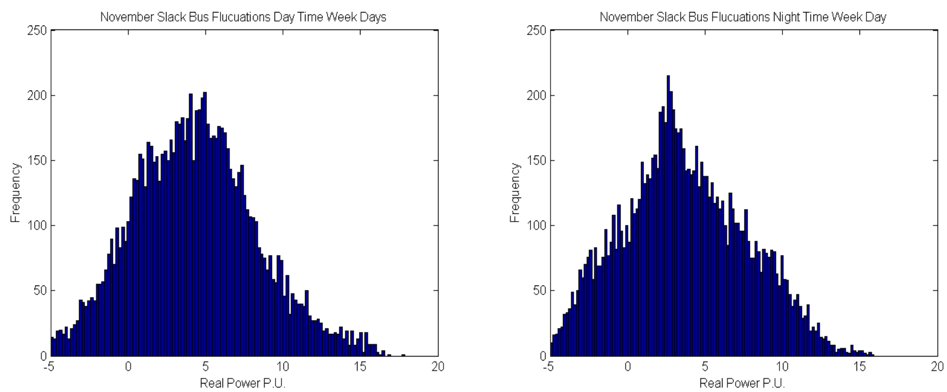

Figure 4.8: Slack bus fluctuation histograms using daytime (left) and nighttime (right) load distributions

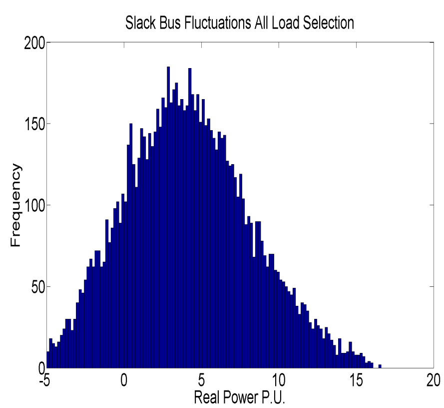

Figure 4.9: Slack bus fluctuation histogram using the full load distribution

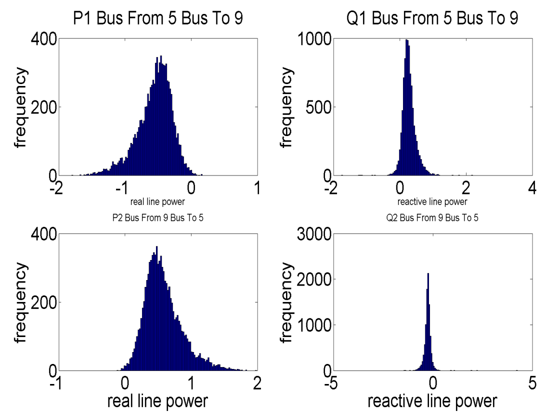

Figure 4.10: Line powers from bus 5 to bus 9 histograms using upper potion of the load distribution

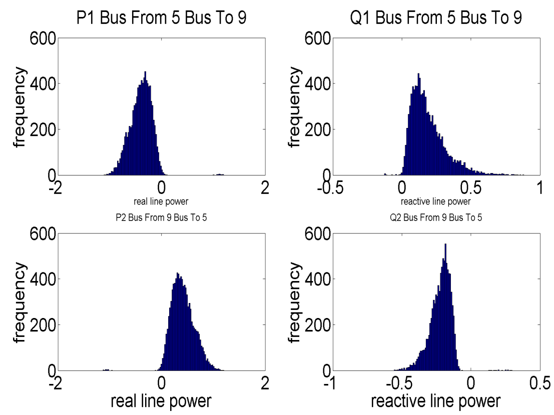

Figure 4.11: Line powers from bus 5 to bus 9 histograms using lower portion of load distribution

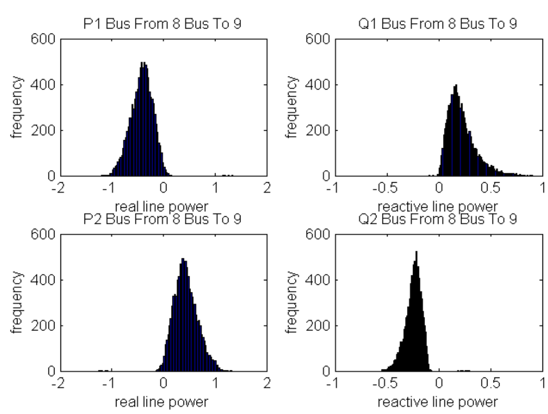

Figure 4.12: Line powers from bus 5 to bus 9 histogram using full load distribution

4.2 Economic Dispatch

In the more realistic scenario with economic dispatch implemented, the voltage results are similar to those found in load flow; refer to Table 4.3. However the combination of the DWD and NWD scenarios produces the largest number of failed to converge simulations. The line powers on the other hand, see Table 4.4, have opposite results than the traditional load flow model, as a result of allowing the other generators to fluctuate and placing the slack bus at a different location (the most expensive generator). The LWD scenario produces the lowest average and second lowest standard deviation, while the UWD scenario produces the second lowest average and lowest standard deviation.

Table 4.5 displays the average and standard deviations of each generator, along with the percentage of the time the generator is at its rated maximum and minimum values. The LWD scenario results with the lowest means and standard deviations, and largest amount of generators running at their minimum. The UWD scenario results with the largest means and standard deviation, and largest amount of generators running at their maximum. Only the nuclear plants have small standard deviations since they are at or close to their maximum value a majority of the time. The other scenario results lie in between these two results again. This appears be what one would expect. The times that the upper loads exist are the same times the wind speeds are at the lowest, refer to Figure 4.13. Thus, revealing that a grid with large loads and low wind generation yields less conclusive results than a grid with low loads and high wind generation. Figures 4.14 through 4.19 display the fluctuations of three selected generators using UWD, LWD and AWD scenarios to help demonstrate the fluctuations the most expensive, mid cost, and cheapest generators will have to meet. Notice in Figure 4.14 and 4.17 the most expensive/last resort generator has to reach values up to 8 p.u. In terms of reality this is impractical and another generator would have to be added to the system.

Both of wind farms real power output is similar to that shown in Figure 3.18 but scaled up to simulate an entire wind farm. The reactive power, however, takes on another form, and due to the reactive power limitations the wind turbines reactive power for one wind farm is always at the maximum value due to its location and surroundings, where as the other wind farm rarely reaches these limits and has a wider range of reactive power. Figures 4.20 and 4.21 display the reactive power output from the two wind farms for the lower load scenario. The combination of the histograms in Figure 4.21 displays the entire reactive power output from the wind farm. Lastly, the voltages and phase angles are plotted in Figures 4.22 through 4.27. Again decisions will need to be made about the voltages occurring under the rated standard. The phase angles take on a different shape than that shown in load flow. A tighter variance exists in economic dispatch with a more acceptable value, due to the new dispatch of generation.

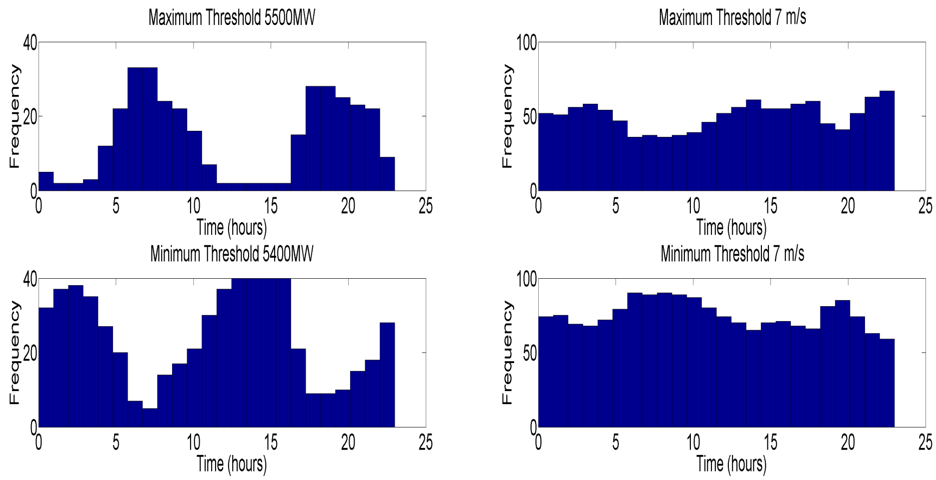

Figure 4.13: Wind speed upper and lower threshold vs load upper and lower threshold

	Scenario	LWD	UWD	DWD	NWD	AWD
Bus 6	σ^2	0.018	0.028	0.026	0.016	0.021
	μ	1.018	1.009	1.007	1.007	1.011
	NERC	1%	2%	2%	1%	1%
Bus 9	σ^2	0.015	0.026	0.024	0.015	0.021
	μ	0.935	0.928	0.925	0.928	0.926
	NERC	9%	39%	20%	25%	26%
Bus 14	σ^2	0.009	0.018	0.014	0.011	0.013
	μ	0.947	0.944	0.943	0.944	0.943
	NERC	2%	8%	6%	2%	3%
	#Failed	6	140	95	0	21
	%Failed	0.05%	1.4%	0.95%	0%	0.21%

Table 4.3: November weekday voltages and failed runs statistics at selected buses

scenario		μ	σ^2	scenario		μ	σ^2
LWD	P1	-0.622	0.316	NWD	P1	-0.879	0.416
	Q1	0.319	0.123		Q1	0.425	0.185
	P2	0.695	0.341		P2	0.937	0.463
	Q2	-0.276	0.043		Q2	-0.281	0.048
	S	0.737	0.335		S	0.979	0.450
UWD	P1	-0.623	0.285	AWD	P1	-0.844	0.409
	Q1	0.321	0.200		Q1	0.416	0.218
	P2	653	0.307		P2	0.899	0.456
	Q2	-0.284	0.171		Q2	-0.286	0.109
	S	0.718	0.310		S	0.948	0.451
DWD	P1	-0.826	0.399				
	Q1	0.414	0.255				
	P2	-0.879	0.443				
	Q2	-0.290	0.137				
	S	0.936	0.451				

Table 4.4: Line powers for each scenario connecting bus 5 to 9

Bus Number	scenario	LWD	UWD	DWD	NWD	AWD
13	μ	0.743	1.0403	1.346	0.942	1.197
	σ^2	1.508	2.023	1.949	1.600	1.831
	max %	9	19	17	11	14
	min %	68	51	46	55	48
2	μ	0.819	1.81	1.180	1.042	1.146
	σ^2	0.771	0.784	0.835	0.839	0.832
	max %	29	50	54	43	49
	min %	34	20	28	31	26
7	μ	1.941	2.302	1.849	1.683	1.804
	σ^2	0.799	0.635	0.880	0.869	0.870
	max %	53	74	51	40	48
	min %	0	0	1	1	1
23	μ	6.044	6.713	7.089	7.049	7.100
	σ^2	1.343	0.937	0.446	0.535	0.444
	max %	42	66	85	82	85
	min %	6	1	0	1	0
15	μ	2.191	2.329	2.190	2.165	2.054
	σ^2	0.441	0.211	0.441	0.457	0.486
	max %	86	97	83	79	83
	min %	0	3	0	0	0
18	μ	4.388	4.399	4.351	4.345	4.359
	σ^2	0.112	0.014	0.205	0.259	0.202
	max %	98	100	92	92	93
	min %	0	0	0	1	0
21	μ	4.388	4.399	4.351	4.345	4.359
	σ^2	0.112	0.014	0.205	0.259	0.202
	max %	98	100	92	92	93
	min %	0	0	0	1	0
22	μ	3.262	3.296	3.253	3.248	3.261
	σ^2	0.151	0.047	0.180	0.207	0.167
	max %	94	99	92	90	93
	min %	0	1	0	1	0

Table 4.5: Generator statistics using economic dispatch

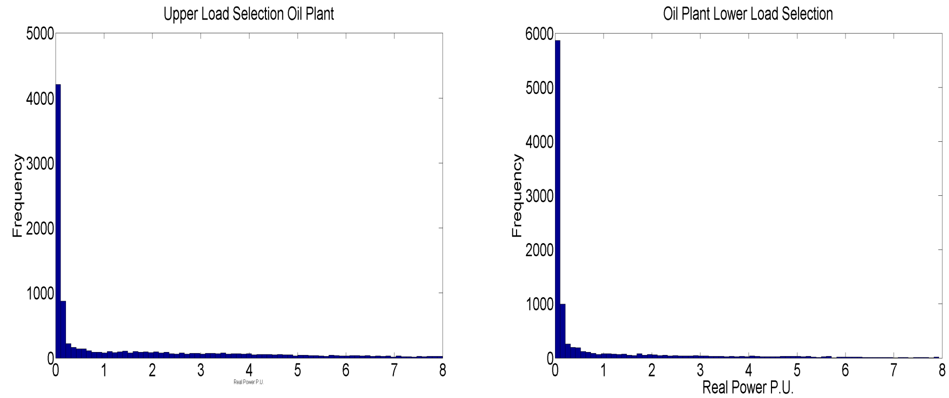

Figure 4.14: Generation histogram using upper (left) and lower (right) portions of load distribution for most expensive generator (oil plant)

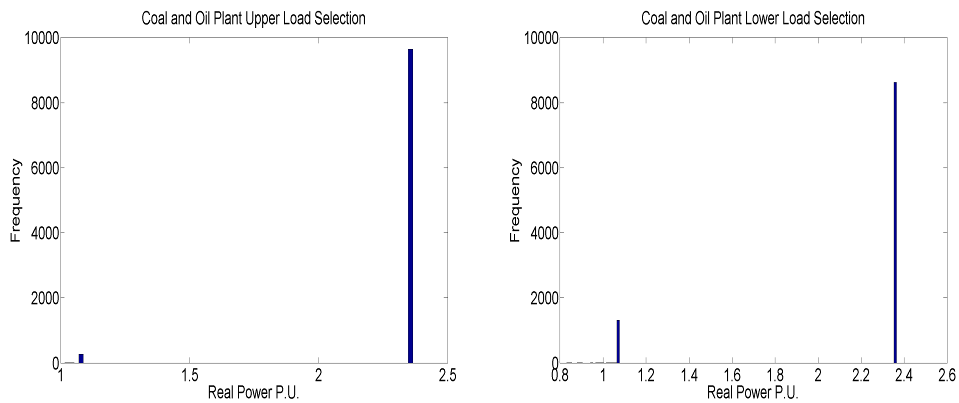

Figure 4.15: Generation histogram using upper (left) and lower (right) portions of load distribution for mid range cost generator (coal and oil plant)

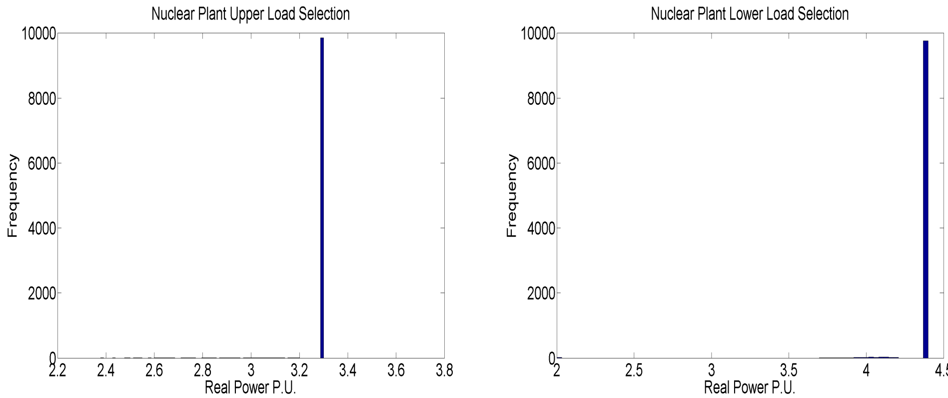

Figure 4.16: Generation histogram using upper (left) and lower (right) portions of load distribution for least expensive generator (nuclear plant)

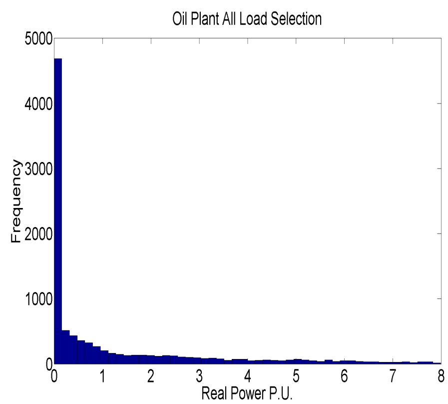

Figure 4.17: Generation histogram using full load distribution for most expensive generator (oil plant)

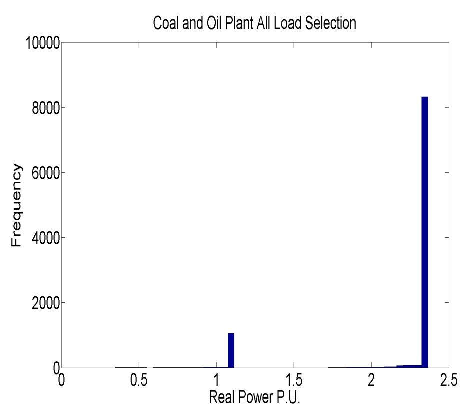

Figure 4.18: Generation histogram using full load distribution for mid range cost generator (coal and oil plant)

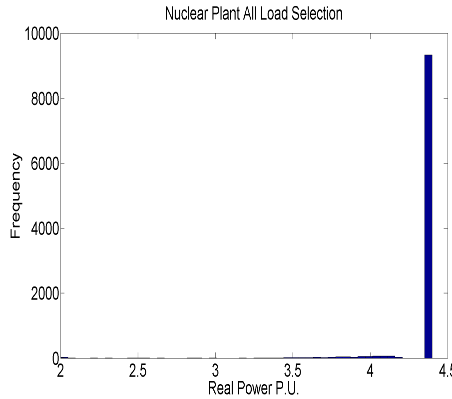

Figure 4.19: Generation histogram using full load distribution for least expensive generator (nuclear plant)

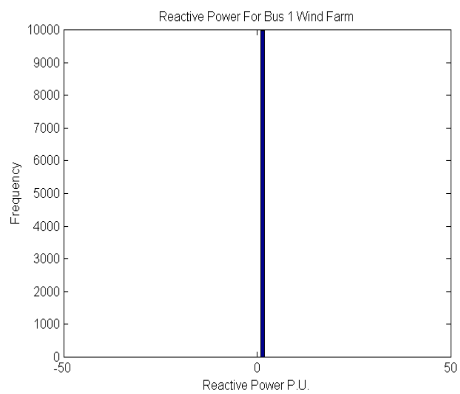

Figure 4.20: Bus 1 PQ conversion via max limits reached, reactive power histogram

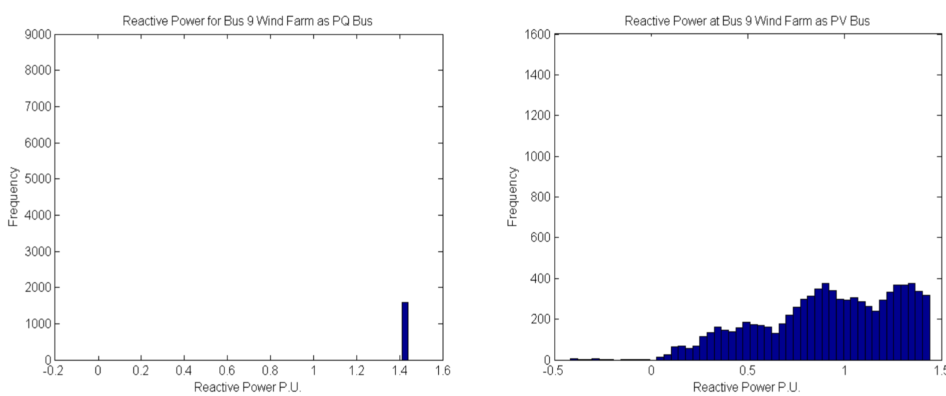

Figure 4.21: Bus 9 PQ bus conversion reactive power via max limits reached and bus 9 PV bus reactive power histogram

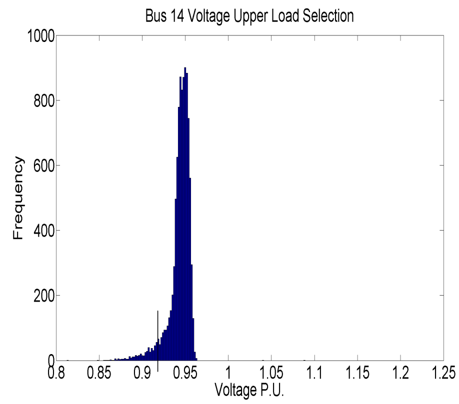

Figure 4.22: Bus 14 voltage histogram using upper portion of load distribution

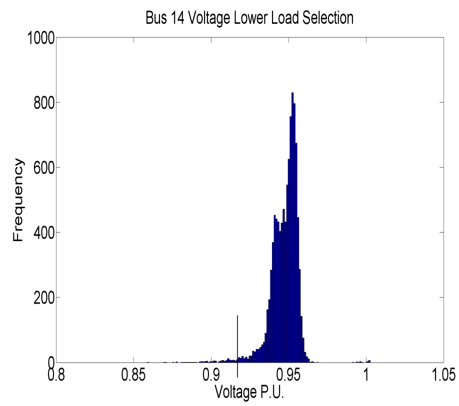

Figure 4.23: Bus 14 voltage histogram using lower portion of load distribution

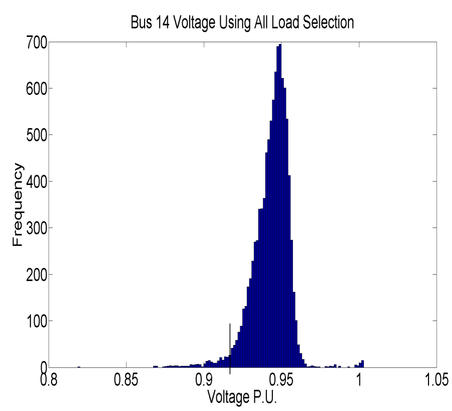

Figure 4.24: Bus 14 voltage histogram using the full load distribution

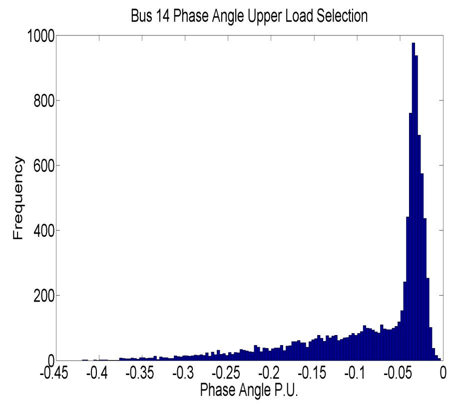

Figure 4.25: Bus 14 phase angle histogram using upper portion of load distribution

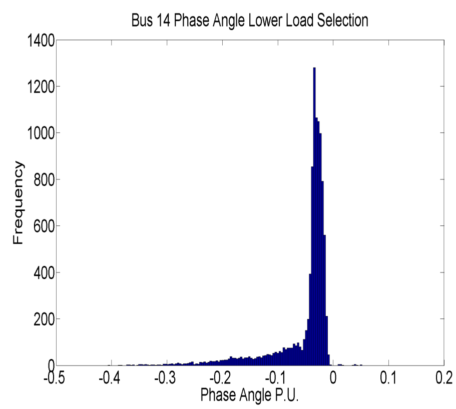

Figure 4.26: Bus 14 phase angle histogram angle using lower portion of load distribution

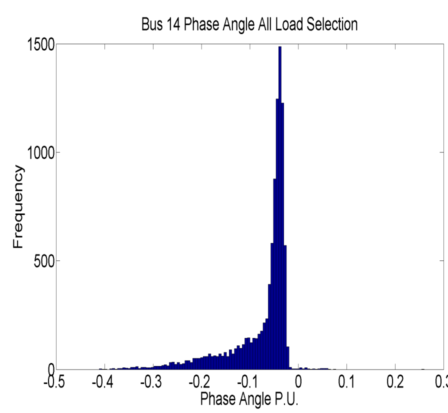

Figure 4.27: Bus 14 phase angle histogram using the full load distribution

The results from traditional load flow and economic dispatch are highly dependent on which generator or generators are being dispatched. The voltage, line power, and phase angle distributions change based on the dispatched generators' locations and how much each generator is being used. Traditional load flow can be thought of as a form of economic dispatch where only one generator responds to the power mismatch between renewable sources and loads, and the other generators are run at a fixed power production. The results from the solutions found from load flow using economic dispatch predict how much each generator is being used, and in turn dictate all power flows through the network. System planners and operators can look at how often the unwanted conditions exist, and decide if it is necessary to perform load curtailment or if additional equipment is needed, such as a capacitor bank for power factor correction, or an additional transmission line to eliminate congestion.

In addition to the afore mentioned uses of load flow with economic dispatch, other aspects of power system operation can be incorporate via the cost function, such as minimizing line losses. Constraints can be added to solutions such that voltages fall within the national standards, phase angles differences between buses remain low, and lines are operated at less than their loadability and thermal limits. Load flow with economic dispatch and constrained solutions lead to optimal power flow. Optimal power flow may cause the system to run inefficiently with regards to cost, but effectively with respect to stability and operating conditions. System planners and operators would use this information to optimize the power grid with respect to having suitable conditions at the lowest possible price.

5 Conclusion

In this report probabilistic load flow with economic dispatch and the proposed random variable selection was proposed as a tool for system planning. The resulting distributions show that by taking specific intervals of wind and load data separated by size, the variance of the solution decreases for one of the proposed scenarios implying more conclusive results. However, this method tends to yield worse conditions when the difference between wind generation and load consumption is high. The percentage of bus voltages and phase angles found above or below the acceptable national values can help system planners make decisions such as incorporating power factor control, voltage control, or reroute power. The voltage distributions found using load flow and economic dispatch are very similar, where as the phase angle between both methods take on completely different statistics and distributions. The phase angle in economic dispatch predicts more desirable results with a narrower variance for all scenarios. The same idea is performed for the percentage of line powers above the lines rated thermal and loadability limits. System planners can then decide if the power should be rerouted or if another line should be placed in parallel. In addition, the variance of the power output of the slack bus or generators under load flow and economic dispatch gives a measure of how widely their power outputs will need to fluctuate and if there are any cases where more generation would need to be installed.

When solving the power flow equations with economic dispatch the voltages, phase angles, and line powers are highly affected by the selection of the cost functions and location of the slack bus. An extension to power flow with economic dispatch is optimal power flow where cost functions can be selected to achieve a variety of objectives based upon economics and performance. Through trial and error load flow with economic dispatch can be used to find a system with desirable conditions where optimal power flow yields desirable solutions after one simulation.

6 Future Work

An extension to the work presented is implementing optimal power flow. In addition to economic dispatch, optimal power flow sets constraints on the power flow solutions in order to create a system with voltages inside the national standards, phase angle differences between buses that are low, and line power less than their loadability and thermal limits, along with minimizing the price of power production. Optimal power flow achieves a solution by curtailing and dispatching generators until the network configuration creates desirable conditions. Economic dispatch can be used to find a system with desirable conditions through trial and error where optimal power flow yields desirable solutions after one simulation.

Optimal power flow uses the analysis performed in this report, load flow with economic dispatch, but in addition sets inequality constraints to voltages, phase angles, and line powers, to solve the power balance equations.

References

[1] R. Allan, C. Grigg, and D. Newey, “Probabilistic analysis of power flows,” *Proceeding of the Institution of Electrical Engineers*, vol. 121, no. 12, pp. 1551–1556, 1974.

[2] B. Borkowska, “Probabilistic load flow,” *Power App. Syst*, pp. 752–759, May 1974.

[3] R. Allan, A. D. Silva, and R. Burchett, “Evaluation methods and accuracy in probabilistic load flow solutions,” *IEEE Trans.*, vol. 5, pp. 2539–2546, May 1981.

[4] J. Morales and J. Perez-Ruiz, “Point estimate schemes to solve the probabilistic power flow,” *IEEE Trans. on Power Systems*, vol. 22, Nov. 2007.

[5] C. Su, “Probabilistic Load-Flow computation using point estimate method,” *IEEE Trans. on Power Systems*, vol. 20, Nov. 2005.

[6] V. Miranda and J. Saraiva, “Fuzzy modelling of power system optimal power flow,” (Baltimore, USA), 1991.

[7] J. Usaola, “Probabilistic load flow with correlated wind power injections,” *Electric Power Systems Research*, vol. 80, no. 5, pp. 528–536, 2010.

[8] A. L. da Silva, V. Arienti, and R. Allan, “Probabilistic load flow considering dependence between input nodal powers,” *IEEE Trans. on Power Apparaturs and Systems*, vol. PAS-103, June 1984.

[9] S. Papathanassiou and N. Boulaxis, “Power limitations and energy yield evaluation for wind farms operating in island systems,” *Renewable energy*, vol. 31, no. 4, pp. 457–479, 2006.

[10] V. Vittal and J. M. U. Shanbhag, “Impact of increased DFIG wind penetration on power systems and markets,” *PSERC Publication 09*, vol. 10, Oct. 2009.

[11] K. Clark, N. Miller, and J. Sanchez-Gasca, “Modeling of GE wind turbine-generators for grid studies,” *GE-Power Systems Energy Consulting, General Electric International, Inc., Schenectady, NY, Tech. Rep.,[Online]. Available: http://www. gepower. com/prod_serv/products/utility_software/en/downloads/09100_Modeling_of_GE_Wind_Turbine-Generators_for_Grid_Studies. pdf*, 2009.

[12] P. Crucitti, V. Latora, and M. Marchiori, “Model for cascading failures in complex networks,” *PHYSICAL REVIEW E*, vol. 69, Apr. 2004.

[13] D. Shin, J. Kim, K. Kim, and C. Singh, “Probabilistic approach to available transfer capability calculation,” *Electric power systems research*, vol. 77, no. 7, pp. 813—820, 2007.

[14] G. Papaefthymiou, P. Schavemaker, and L. van der Sluis, “Survey on the modelling of the uncertainty in distributed power systems,” *IEEE Young Researchers Symposium, Delft, the Netherlands*, 2004.

[15] J. Glover, M. Sarma, and T. Overbye, "Power systems analysis and design," 2008.

[16] C. Grigg, P. Wong, P. Albrecht, R. Allan, M. Bhavaraju, R. Billinton, Q. Chen, C. Fong, S. Haddad, S. Kuruganty, *et al.*, "The IEEE reliability test system-1996. A report prepared by the reliability test system task force of the application of probability methods subcommittee," *Power Systems, IEEE Transactions on*, vol. 14, no. 3, pp. 1010–1020, 1999.

[17] R. Hogg and A. Craig, "Introduction to mathematical statistics," 1994.

[18] H. Alder and E. Roessler, "Introduction to Probability and Statistics. San Francisco: W. H," 1968.

[19] G. Energy, "2.5 MW wind turbine: A production of ecomagination," *General Electric Company*, 2008.

[20] M. Seyedi, *Evaluation of the DFIG Wind Turbine Built-in Model in PSS/E*. PhD thesis, Chalmers, Goteborg, Sweden, June 2009.

7 Appendix

7.1 List of Acronyms

UWD	Upper load threshold weekday
UWE	Upper load threshold weekend
LWD	Lower load threshold weekday
LWE	Lower load threshold weekend
DWD	Day time load weekday
DWE	Day time load weekend
NWD	Night time load weekday
NWE	Night time load weekend
AWD	All load times weekday
AWE	All load times weekend
AAT	All load times All Days

7.2 Admittance Matrix for Modified IEEE 24-bus System

bus	admittance	bus	admittance	bus	admittance	bus	admittance
1,1	0.015 - 0.110i	4,1	-0.001 + 0.011i	19,1	-0.001 + 0.010i	23,1	-0.012 + 0.089i
2,2	0.117 - 1.070i	9,2	-0.015 + 0.068i	12,2	-0.002 + 0.007i	14,2	-0.001 + 0.004i
26,2	-0.099 + 0.990i	3,3	0.103 - 1.005i	15,3	-0.004 + 0.015i	27,3	-0.099 + 0.990i
1,4	-0.001 + 0.011i	4,4	0.105 - 1.042i	18,4	-0.003 + 0.020i	19,4	-0.003 + 0.020i
28,4	-0.099 + 0.990i	5,5	0.113 - 1.107i	7,5	-0.005 + 0.040i	10,5	-0.007 + 0.058i
24,5	-0.003 + 0.018i	29,5	-0.099 + 0.991i	6,6	0.118 - 1.135i	7,6	-0.009 + 0.075i
21,6	-0.010 + 0.070i	31,6	-0.099 + 0.991i	5,7	-0.005 + 0.040i	6,7	-0.009 + 0.075i
7,7	0.016 - 0.130i	8,7	-0.002 + 0.014i	7,8	-0.002 + 0.014i	8,8	0.003 - 0.023i
21,8	-0.001 + 0.009i	2,9	-0.015 + 0.068i	9,9	0.118 - 1.073i	11,9	-0.001 + 0.004i
13,9	-0.003 + 0.011i	25,9	-0.099 + 0.990i	5,10	-0.007 + 0.058i	10,10	0.117 - 1.145i
20,10	-0.001 + 0.016i	21,10	-0.004 + 0.038i	22,10	-0.006 + 0.042i	30,10	-0.099 + 0.990i
9,11	-0.001 + 0.004i	11,11	0.004 - 0.024i	16,11	-0.002 + 0.007i	24,11	-0.001 + 0.011i
2,12	-0.002 + 0.007i	12,12	0.004 - 0.016i	16,12	-0.002 + 0.009i	9,13	-0.003 + 0.011i
13,13	0.006 - 0.021i	17,13	-0.003 + 0.010i	2,14	-0.001 + 0.004i	14,14	0.005 - 0.019i
17,14	-0.004 + 0.015i	3,15	-0.004 + 0.015i	15,15	0.007 - 0.026i	16,15	-0.002 + 0.005i
17,15	-0.002 + 0.005i	11,16	-0.002 + 0.007i	12,16	-0.002 + 0.009i	15,16	-0.002 + 0.005i
16,16	0.006 - 0.046i	18,16	-0.001 + 0.011i	19,16	-0.001 + 0.011i	13,17	-0.003 + 0.010i
14,17	-0.004 + 0.015i	15,17	-0.002 + 0.005i	17,17	0.008 - 0.054i	18,17	-0.001 + 0.011i
19,17	-0.001 + 0.011i	4,18	-0.003 + 0.020i	16,18	-0.001 + 0.011i	17,18	-0.001 + 0.011i
18,18	0.006 - 0.067i	20,18	-0.003 + 0.023i	1,19	-0.001 + 0.010i	4,19	-0.003 + 0.020i
16,19	-0.001 + 0.011i	17,19	-0.001 + 0.011i	19,19	0.004 - 0.054i	10,20	-0.001 + 0.016i
18,20	-0.003 + 0.023i	20,20	0.004 - 0.040i	6,21	-0.010 + 0.070i	8,21	-0.001 + 0.009i
10,21	-0.004 + 0.038i	21,21	0.016 - 0.117i	10,22	-0.006 + 0.042i	22,22	0.012 - 0.091i
23,22	-0.006 + 0.049i	1,23	-0.012 + 0.089i	22,23	-0.006 + 0.049i	23,23	0.018 - 0.138i
5,24	-0.003 + 0.018i	11,24	-0.001 + 0.011i	24,24	0.003 - 0.030i	9,25	-0.099 + 0.990i
25,25	0.099 - 0.990i	2,26	-0.099 + 0.991i	26,26	0.099 - 0.990i	3,27	-0.099 + 0.990i
27,27	0.099 - 0.990i	4,28	-0.099 + 0.991i	28,28	0.099 - 0.990i	5,29	-0.099 + 0.990i
29,29	0.099 - 0.990i	10,30	-0.099 + 0.991i	30,30	0.099 - 0.990i	6,31	-0.099 + 0.990i
31,31	0.099 - 0.990i						